mitochondrial fission (Fis1, Drp1) and fusion genes (Mfn1, Mfn2, OPA1). Real-time PCR analysis showed that each gene expression was not significantly altered by TBT exposure (Fig. 3A). Fusion allows damaged mitochondria to incorporate into intact mitochondria, thereby maintaining mitochondrial function.[30] Dysfunctional mitochondria may lose their fusion capacity by the degradation of fusion proteins, resulting in the accumulation of fragmented mitochondria. Thus, we assessed the protein expression of Mfn1, Mfn2, and OPA1 in the presence or absence of TBT. Western blot analysis revealed that Mfn1 and Mfn2 protein levels were significantly reduced after 6 h, whereas OPA1 protein expression was not changed after 24 h (Fig. 3B and C). The other mitochondrial inner membrane protein, cytochrome *c* oxidase subunit IV (COX IV), was also not changed after 24 h (Fig. 3B). Moreover, MG132, a proteasome inhibitor, recovered the TBT-induced reduction in Mfn1 and Mfn2 (Fig. 3C). In contrast, the fusion proteins Fis1 and Drp1 were not affected by TBT (Fig. 3D). These data suggest that TBT-induced mitochondrial fragmentation is caused by the proteasomal degradation of Mfn1 and Mfn2.

Consistent with our data, chemical stressors have been reported to cause mitochondrial fission through the proteasomal degradation of Mfn. For example, doxorubicin induces ubiquitin-mediated proteasomal degradation of Mfn2, which facilitates mitochondrial fragmentation and apoptosis in sarcoma U2OS cells.[31] Another study has shown that CGP37157, an inhibitor of mitochondrial calcium efflux, mediates mitochondrial fission through Mfn1 degradation *via* ubiquitin ligase in prostate cancer LNCaP cells.[32] Since it remains unknown if ubiquitin ligases are involved or not in these TBT actions, further studies should be addressed to clarify the TBT-induced mechanism of proteasomal degradation of Mfn1 and Mfn2.

TBT induces mitochondrial defects *via* NAD-IDH

To investigate whether Mfn degradation and mitochondrial dysfunction are mediated through the non-genomic TBT target NAD-IDH, we examined the effects of apigenin, an NAD-IDH inhibitor,[33] on mitochondrial function. Apigenin (10 μM) decreased the number of cells undergoing mitochondrial fusion and induced mitochondrial fragmentation after 24 h (Fig. 4A and B). Furthermore, apigenin significantly reduced Mfn1 and Mfn2 protein expression, which was recovered by MG132 treatment (Fig. 4C). Apigenin has been reported to inhibit not only NAD-IDH but also hnRNPA2 and NF-κB.[33]

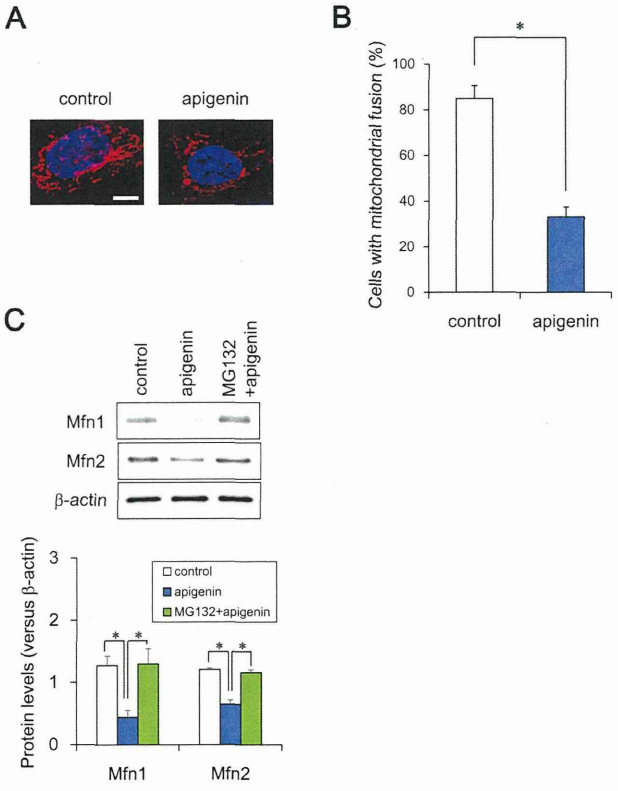

Fig. 4 Effect of apigenin on mitochondrial function in NT2/D1 cells. Cells were exposed to 10 μM apigenin. (A) Cells were stained with MitoTracker Red CMXRos and DAPI. Mitochondrial morphology was observed by confocal laser microscopy. Bar = 10 μm. (B) The number of cells undergoing mitochondrial fusion (<10% punctiform) was counted in each image. Data represent mean ± s.d. (n = 5). (C) Mitochondrial proteins in the cell lysate were analyzed by western blotting using anti-Mfn1 or Mfn2 antibodies. Data represent mean ± s.d. (n = 3). *P < 0.05.

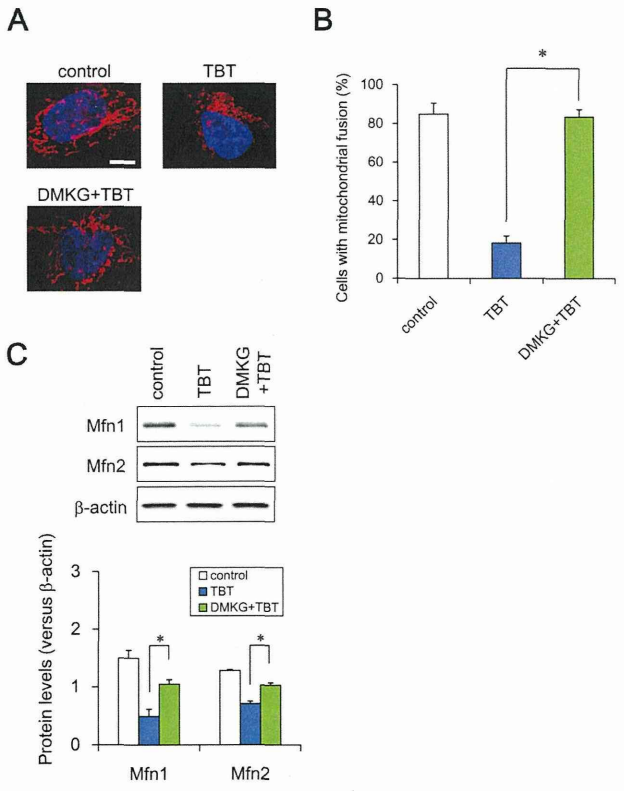

Fig. 5 Effect of DMKG on TBT-induced mitochondrial dysfunctions in NT2/D1 cells. Cells were exposed to 100 nM TBT and 7 mM DMKG. (A) Cells were stained with MitoTracker Red CMXRos and DAPI. Mitochondrial morphology was observed by confocal laser microscopy. Bar = 10 μm. (B) The number of cells undergoing mitochondrial fusion (<10% punctiform) was counted in each image. Data represent mean ± s.d. (n = 5). (C) Mitochondrial proteins were analyzed by western blotting using anti-Mfn1 or Mfn2 antibodies. Data represent mean ± s.d. (n = 3). *P < 0.05.

We cannot rule out the possibility that apigenin-induced mitochondrial dysfunction was induced by other targets. It is necessary to confirm our data by shRNA against NAD-IDH. To further confirm the involvement of NAD-IDH, we used dimethyl α-ketoglutarate (DMKG), a cell-permeable analog of α-ketoglutarate.[34] Incubation with DMKG prevented TBT-induced mitochondrial fragmentation in NT2/D1 cells (Fig. 5A) and recovered the number of cells undergoing mitochondrial fusion to the basal level (Fig. 5B). Furthermore, DMKG significantly recovered the TBT-induced the proteasomal degradation of Mfn1 and Mfn2 (Fig. 5C). Taken together, these data suggest that NAD-IDH mediates TBT-induced mitochondrial dysfunction *via* Mfn degradation in NT2/D1 cells. In addition to NAD-IDH, citrate synthase and α-ketoglutarate dehydrogenase also work as rate-limiting enzymes in the TCA cycle. Aluminium has been shown to induce oxidative stress *via* the negative regulation of citrate synthase and α-ketoglutarate dehydrogenase.[35,36] We could not rule out the possibility that TBT affects these enzymes. Several reports indicate that knockdown of Mfn1 and Mfn2 in the cells induces mitochondrial fragmentation and shows severe cellular defects, including decreased ATP content and poor cell growth.[30,37] Especially, Mfn2 has been reported to be necessary for striatal axonal projections of midbrain dopamine neurons by studies using dopamine neuron-specific Mfn2 knockout mice.[38] Taken together, Mfn1 and Mfn2 might be involved in several TBT actions *via* NAD-IDH, such as the reduction of ATP content, growth inhibition and enhancement of neuronal differentiation.

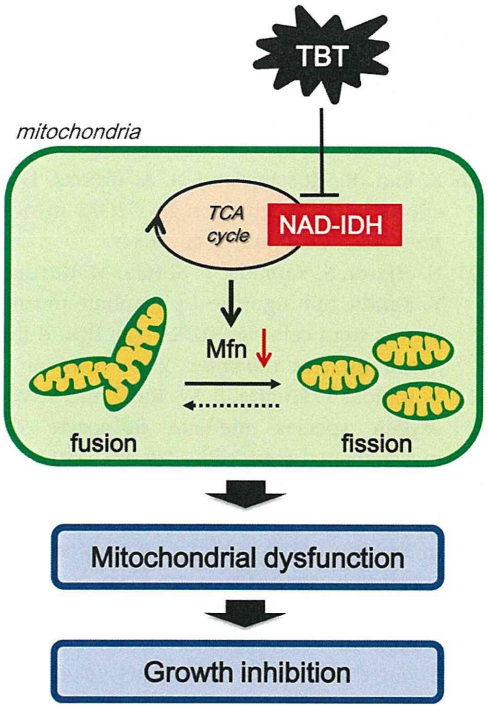

Fig. 6 Proposed model of TBT toxicity through non-genomic pathways in human embryonic carcinoma cells. Nanomolar TBT levels induce Mfn degradation and mitochondrial fission through NAD-IDH inhibition. These negative effects of TBT on mitochondrial quality control could mediate cell growth inhibition.

Conclusions

Based on our data, we have proposed a model of nanomolar TBT-induced mitochondrial dysfunction in neuronal precursor cells (Fig. 6). We demonstrated that TBT mediates the inhibition of NAD-IDH and the loss of mitochondrial quality control, representing a novel non-genomic pathway of TBT-induced toxicity. These negative effects of TBT on mitochondria could inhibit ATP production and cell growth. Since TBT at micromolar levels is known to cause neuronal degeneration *via* multiple mitochondrial defects, similar mitochondrial dysfunction might be also observed in immature neuronal precursor cells. We have previously revealed TBT-induced NAD-IDH inhibition in the rat brain. It would be interesting to study whether TBT-induced mitochondrial dysfunction *via* NAD-IDH might be also observed *in vivo*. We are now conducting experiments to determine how TBT degrades Mfn proteins both *in vitro* and *in vivo*. It remains to be determined if micromolar concentrations of TBT induce other mitochondrial dysfunctions in NT2/D1 cells and if the mechanisms pointed out here are selective for immature cells.

List of abbreviations

CCCP	Carbonylcyanide *m*-chlorophenylhydrazone
CHX	Cycloheximide
COX IV	Cytochrome *c* oxidase subunit IV
DAPI	4′,6-Diamidino-2-phenylindole
DMEM	Dulbecco's modified Eagle's medium
DMKG	Dimethyl α-ketoglutarate
Drp1	Dynamin-related protein 1
FBS	Fetal bovine serum
Fis1	Fission protein 1
GAPDH	Glyceraldehyde-3-phosphate dehydrogenase
Mfn	Mitofusin
NAD-IDH	NAD^+-dependent isocitrate dehydrogenase
Opa1	Optic atrophy 1
PPAR	Peroxisome proliferator activated receptor
RGZ	Rosiglitazone
RXR	Retinoid X receptor
TA	Tin acetate
TBT	Tributyltin
TCA	Tricarboxylic acid

Conflict of interest

The authors declare that there are no conflicts of interest.

Acknowledgements

This work was supported by a Health and Labour Sciences research grant from the Ministry of Health, Labour and Welfare, Japan (#H25-Kagaku-Ippan-002 to Y.Ka.), a grant-in-aid for scientific research from the Ministry of Education, Culture, Sports, Science, and Technology, Japan (#26293056, #26670041 to Y. Kanda), and a grant from the Smoking Research Foundation (Y. Kanda).

References

1 E. Dopp, L. M. Hartmann, A. M. Florea, A. W. Rettenmeier and A. V. Hirner, Environmental distribution, analysis, and toxicity of organometal(loid) compounds, *Crit. Rev. Toxicol.*, 2004, **34**, 301–333.

2 A. T. Gardlund, T. Archer, K. Danielsen, B. Danielsson, A. Frederiksson, N. G. Lindquist, H. Lindstrom and J. Luthman, Effects of prenatal exposure to tributyltin and trihexyltin on behavior in rats, *Neurotoxicol. Teratol.*, 1991, **13**, 99–105.

3 A. Mariani, R. Fanelli, A. Re Depaolini and M. De Paola, Decabrominated diphenyl ether and methylmercury impair fetal nervous system development in mice at documented human exposure levels, *Dev. Neurobiol.*, 2015, **75**, 23–38.

4 G. Winneke, Developmental aspects of environmental neurotoxicology: lessons from lead and polychlorinated biphenyls, *J. Neurol. Sci.*, 2011, **308**, 9–15.

5 L. G. Costa, M. Aschne, A. Vitalone, T. Syversen and O. P. Soldin, Developmental neuropathology of environmental agents, *Annu. Rev. Pharmacol. Toxicol.*, 2004, **44**, 87–110.

6 J. Dobbing, Vulnerable periods in developing brain, in *Appl. Neurochem*, ed. A. N. Davison and J. Dobbing, Davis, Philadelphia, 1968, pp. 287–316.

7 P. M. Rodier, Developing brain as a target of toxicity, *Environ. Health Perspect.*, 1995, **103**(suppl 6), 73–76.

8 T. Kanayama, N. Kobayashi, S. Mamiya, T. Nakanishi and J. Nishikawa, Organotin compounds promote adipocyte differentiation as agonists of the peroxisome proliferator-activated receptor gamma/retinoid X receptor pathway, *Mol. Pharmacol.*, 2005, **67**, 766–774.

9 M. Kajta and A. K. Wójtowicz, Impact of endocrine-disrupting chemicals on neural development and the onset of neurological disorders, *Pharmacol. Rep.*, 2013, **65**, 1632–1639.

10 H. S. Elsabbagh, S. Z. Moussa and O. S. El-tawil, Neurotoxicologic sequelae of tributyltin intoxication in rats, *Pharmacol. Res.*, 2002, **45**, 201–206.

11 S. Nesci, V. Ventrella, F. Trombetti, M. Pirini and A. Pagliarani, Tributyltin (TBT) and mitochondrial respiration in mussel digestive gland, *Toxicol. in Vitro*, 2011, **25**, 951–959.

12 S. Nesci, V. Ventrella, F. Trombetti, M. Pirini, A. R. Borgatti and A. Pagliarani, Tributyltin (TBT) and dibutyltin (DBT) differently inhibit the mitochondrial Mg-ATPase activity in mussel digestive gland, *Toxicol. in Vitro*, 2011, **25**, 117–124.

13 Y. Nakatsu, Y. Kotake, N. Takai and S. Ohta, Involvement of autophagy *via* mammalian target of rapamycin (mTOR) inhibition in tributyltin-induced neuronal cell death, *J. Toxicol. Sci.*, 2010, **35**, 245–251.

14 Y. Kotake, Molecular mechanisms of environmental organotin toxicity in mammals, *Biol. Pharm. Bull.*, 2012, **35**, 1876–1880.

15 S. Mitra, R. Gera, W. A. Siddiqui and S. Khandelwal, Tributyltin induces oxidative damage, inflammation and apoptosis *via* disturbance in blood–brain barrier and metal homeostasis in cerebral cortex of rat brain: an *in vivo* and *in vitro* study, *Toxicology*, 2013, **310**, 39–52.

16 M. Bani-Yaghoub, J. M. Felker and C. C. Naus, Human NT2/D1 cells differentiate into functional astrocytes, *NeuroReport*, 1999, **10**, 3843–3846.

17 S. Yamada, Y. Kotake, Y. Sekino and Y. Kanda, AMP-activated protein kinase-mediated glucose transport as a novel target of tributyltin in human embryonic carcinoma cells, *Metallomics*, 2013, **5**, 484–491.

18 S. Yamada, Y. Kotake, Y. Demizu, M. Kurihara, Y. Sekino and Y. Kanda, NAD-dependent isocitrate dehydrogenase as a novel target of tributyltin in human embryonic carcinoma cells, *Sci. Rep.*, 2014, **4**, 5952.

19 C. M. Nasrallah and T. L. Horvath, Mitochondrial dynamics in the central regulation of metabolism, *Nat. Rev. Endocrinol.*, 2014, **10**, 650–658.

20 R. J. Youle and A. M. van der Bliek, Mitochondrial fission, fusion, and stress, *Science*, 2012, **337**, 1062–1065.

21 T. Koshiba, S. A. Detmer, J. T. Kaiser, H. Chen, J. M. McCaffery and D. C. Chan, Structural basis of mitochondrial tethering by mitofusin complexes, *Science*, 2004, **305**, 858–862.

22 S. Cipolat, O. M. De Brito, B. Dal Zilio and L. Scorrano, OPA1 requires mitofusin 1 to promote mitochondrial fusion, *Proc. Natl. Acad. Sci. U. S. A.*, 2004, **101**, 15927–15932.

23 H. Chen, S. A. Detmer, A. J. Ewald, E. Erik, S. E. F. Griffin and D. C. Chan, Mitofusins mfn1 and mfn2 coordinately regulate mitochondrial fusion and are essential for embryonic development, *J. Cell Biol.*, 2003, **160**, 189–200.

24 E. Smirnova, L. Griparic, D.-L. Shurland and A. M. van der Bliek, Dynamin-related protein Drp1 is required for mitochondrial division in mammalian cells, *Mol. Biol. Cell*, 2001, **12**, 2245–2256.

25 Y. Yoon, E. W. Krueger, B. J. Oswald and M. A. McNiven, The mitochondrial protein hFis1 regulates mitochondrial fission in mammalian cells through an interaction with the dynamin-like protein DLP1, *Mol. Biol. Cell*, 2003, **23**, 5409–5420.

26 X. Fan, R. Hussien and G. A. Brooks, H_2O_2-induced mitochondrial fragmentation in C2C12 myocytes, *Free Radical Biol. Med.*, 2010, **49**, 1646–1654.

27 N. Hiarta, S. Yamada, T. Shoda, M. Kurihara, Y. Sekino and Y. Kanda, Sphingosine-1-phosphate promotes expansion of cancer stem cells *via* S1PR3 by a ligand-independent Notch activation, *Nat. Commun.*, 2014, **5**, 4806.

28 Y. Kanda, T. Hinara, S. W. Kang and Y. Watanabe, Reactive oxygen species mediate adipocyte differentiation in mesenchymal stem cells, *Life Sci.*, 2011, **89**, 250–258.

29 A. Tanaka, M. M. Cleland, S. Xu, D. P. Narendra, D. F. Suen, M. Karbowski and R. J. Youle, Proteasome and p97 mediate mitophagy and degradation of mitofusins induced by Parkin, *J. Cell Biol.*, 2010, **191**, 1367–1380.

30 H. Chen, A. Chomyn and D. C. Chan, Disruption of fusion results in mitochondrial heterogeneity and dysfunction, *J. Biol. Chem.*, 2005, **280**, 26185–26192.

31 G. P. Leboucher, Y. C. Tsai, M. Yang, K. C. Shaw, M. Zhou, T. D. Veenstra, M. H. Glickman and A. M. Weissman, Stress-induced phosphorylation and proteasomal degradation of mitofusin 2 facilitates mitochondrial fragmentation and apoptosis, *Mol. Cell*, 2012, **47**, 547–557.

32 V. Choudhary, I. Kaddour-Djebbar, R. Alaisami, M. V. Kumar and W. B. Bollag, Mitofusin 1 degradation is induced by a disruptor of mitochondrial calcium homeostasis, CGP37157: a role in apoptosis in prostate cancer cells, *Int. J. Oncol.*, 2014, **44**, 1767–1773.

33 D. Arango, K. Morohashi, A. Yilmaz, K. Kuramochi, A. Parihar, B. Brahimaj, E. Grotewold and A. I. Doseff, Molecular basis for the action of a dietary flavonoid revealed by the comprehensive identification of apigenin human targets, *Proc. Natl. Acad. Sci. U. S. A.*, 2013, **110**, E2153–E2162.

34 M. Willenborg, U. Panten and I. Rustenbeck, Triggering and amplification of insulin secretion by dimethyl alpha-ketoglutarate, a membrane permeable alpha-ketoglutarate analogue, *Eur. J. Pharmacol.*, 2009, **607**, 41–46.

35 D. R. Sharma, A. Sunkaria, W. Y. Wani, R. K. Sharma, R. J. Kandimalla, A. Bal and K. D. Gill, Aluminium induced oxidative stress results in decreased mitochondrial biogenesis *via* modulation of PGC-1α expression, *Toxicol. Appl. Pharmacol.*, 2013, **273**, 365–380.

36 R. J. Mailloux, J. Lemire and V. D. Appanna, Hepatic response to aluminum toxicity: dyslipidemia and liver diseases, *Exp. Cell Res.*, 2011, **317**, 2231–2238.

37 W. Yue, Z. Chen, H. Liu, C. Yan, M. Chen, D. Feng, C. Yan, H. Wu, L. Du, Y. Wang, J. Liu, X. Huang, L. Xia, L. Liu, X. Wang, H. Jin, J. Wang, Z. Song, X. Hao and Q. Chen, A small natural molecule promotes mitochondrial fusion through inhibition of the deubiquitinase USP30, *Cell Res.*, 2014, **24**, 482–496.

38 S. Lee, F. H. Sterky, A. Mourier, M. Terzioglu, S. Cullheim, L. Olson and N. G. Larsson, Mitofusin 2 is necessary for striatal axonal projections of midbrain dopamine neurons, *Hum. Mol. Genet.*, 2012, **21**, 4827–4835.

The Journal of Toxicological Sciences (J. Toxicol. Sci.)
Vol.41, No.2, 207-215, 2016

Original Article

Tributyltin induces G2/M cell cycle arrest via NAD$^+$-dependent isocitrate dehydrogenase in human embryonic carcinoma cells

Miki Asanagi[1,2,*], Shigeru Yamada[1,*], Naoya Hirata[1], Hiroshi Itagaki[2], Yaichiro Kotake[3], Yuko Sekino[1] and Yasunari Kanda[1]

[1]*Division of Pharmacology, National Institute of Health Sciences, 1-18-1 Kamiyoga, Setagaya-ku, Tokyo 158-8501, Japan*
[2]*Faculty of Engineering, Department of Materials Science and Engineering, Yokohama National University, 79-5 Tokiwadai, Hodogaya-ku, Yokohama, Kanagawa 240-8501, Japan*
[3]*Department of Xenobiotic Metabolism and Molecular Toxicology, Graduate School of Biomedical and Health Sciences, Hiroshima University, 1-2-3 Kasumi, Minami-ku, Hiroshima 734-8553, Japan*

(Received November 16, 2015; Accepted December 28, 2015)

ABSTRACT — Organotin compounds, such as tributyltin (TBT), are well-known endocrine-disrupting chemicals (EDCs). We have recently reported that TBT induces growth arrest in the human embryonic carcinoma cell line NT2/D1 at nanomolar levels by inhibiting NAD$^+$-dependent isocitrate dehydrogenase (NAD-IDH), which catalyzes the irreversible conversion of isocitrate to α-ketoglutarate. However, the molecular mechanisms by which NAD-IDH mediates TBT toxicity remain unclear. In the present study, we examined whether TBT at nanomolar levels affects cell cycle progression in NT2/D1 cells. Propidium iodide staining revealed that TBT reduced the ratio of cells in the G1 phase and increased the ratio of cells in the G2/M phase. TBT also reduced cell division cycle 25C (cdc25C) and cyclin B1, which are key regulators of G2/M progression. Furthermore, apigenin, an inhibitor of NAD-IDH, mimicked the effects of TBT. The G2/M arrest induced by TBT was abolished by NAD-IDHα knockdown. Treatment with a cell-permeable α-ketoglutarate analogue recovered the effect of TBT, suggesting the involvement of NAD-IDH. Taken together, our data suggest that TBT at nanomolar levels induced G2/M cell cycle arrest via NAD-IDH in NT2/D1 cells. Thus, cell cycle analysis in embryonic cells could be used to assess cytotoxicity associated with nanomolar level exposure of EDCs.

Key words: Embryonic carcinoma cells, Tributyltin, Cell cycle, Isocitrate dehydrogenase

INTRODUCTION

Organotin compounds, such as tributyltin (TBT) are typical environmental contaminants and are categorized as endocrine-disrupting chemicals (EDCs), which cause neurodevelopmental defects including behavioral abnormality and teratogenicity (Dopp *et al.*, 2004; Gårdlund *et al.*, 1991). Although the use of TBT has already been restricted, butyltin compounds, including TBT, can still be found in human blood at concentrations between 50 and 400 nM. There is still concern about TBT toxicity for human health (Whalen *et al.*, 1999).

Several studies have revealed that TBT activates retinoid X receptor (RXR) and/or peroxisome proliferator-activated receptor γ (PPARγ) (Kanayama *et al.*, 2005). TBT at nanomolar levels has the ability to bind with higher affinity than the intrinsic ligands and these genomic transcriptional activations have been reported to mediate neurodevelopmental defects in *Xenopus* (Yu *et al.*, 2011). In contrast, TBT elicits non-genomic pathway in mature rat neurons and brain tissues at nearly micromolar levels. For instance, TBT induces neuronal death by inhibiting mammalian target of rapamycin (mTOR) in rat cortical neurons (Nakatsu *et al.*, 2010). TBT also induces neuronal degeneration via the generation of reactive oxygen species along with marked reduction of GSH/GSSG levels in the rat brain (Mitra *et al.*, 2013).

Cell stress is known to trigger a checkpoint that arrests cells in the G1 or G2 phase (Gabrielli *et al.*, 2012). The cell cycle is tightly regulated by spatial and temporal

Correspondence: Yasunari Kanda (E-mail: kanda@nihs.go.jp)
*These authors equally contributed to this work.

expression of cell cycle proteins and divided into p53-dependent and p53-independent regulations (Shackelford *et al.*, 1999). In the p53-independent regulations, cdc25C phosphatase, a mitotic inducer, plays a central role in G2/M phase regulation. Cdc25C activates cyclin B1/cyclin-dependent kinase (Cdk) 1 complex, which triggers mitosis (Donzelli and Draetta, 2003) and cyclin B1 accumulates during the S and G2 phases, followed by nuclear translocation and association with Cdk1. Protein levels of these cell cycle regulators are strictly regulated during cell cycle progression. Ultraviolet irradiation or toxic drugs are known to cause G2 arrest by the inactivation of cyclin B1/Cdk1 via p53 induction followed by the upregulation of p21, a Cdk inhibitor and/or cdc25C downregulation by degradation (Chaudhary *et al.*, 2013; Kawabe, 2004; Nam *et al.*, 2010; Ouyang *et al.*, 2009).

We have previously reported that nanomolar levels of TBT induce growth arrest of neuronal precursor NT2/D1 cells as a model of neurodevelopmental stage (Yamada *et al.*, 2013). We found that TBT causes growth arrest via mitochondrial NAD^+-dependent isocitrate dehydrogenase (NAD-IDH), which catalyzes the irreversible conversion of isocitrate to α-ketoglutarate in the tricarboxylic acid (TCA) cycle (Yamada *et al.*, 2014). Based on these observations, we hypothesized that nanomolar levels of TBT could also affect cell cycle progression via NAD-IDH in NT2/D1 cells.

In the present study, we investigated the effect of TBT on cell cycle progression in NT2/D1 cells. We found that exposure to 100 nM TBT reduced the protein levels of cell cycle regulators and induced G2/M cell cycle arrest through an NAD-IDH-dependent mechanism. Thus, cell cycle regulation via NAD-IDH is a novel target of TBT-induced toxicity in human embryonic carcinoma cells.

MATERIALS AND METHODS

Cell culture

NT2/D1 cells were obtained from the American Type Culture Collection (Manassas, VA, USA). The cells were cultured in Dulbecco's modified Eagle's medium (DMEM; Sigma-Aldrich, St. Louis, MO, USA) supplemented with 10% fetal bovine serum (FBS; Biological Industries, Ashrat, Israel) and 0.05 mg/mL penicillin-streptomycin mixture (Life Technologies, Carlsbad, CA, USA) at 37°C in 5% CO_2.

Cell cycle analysis

The cells were trypsinized and harvested in phosphate buffered saline. Then the cells were resuspended in 70% ethanol for 30 min at -20°C. The fixed cells were collected by centrifugation and resuspended in propidium iodide (PI)/RNase Staining Buffer (BD Biosciences, San Jose, CA, USA) followed by incubation at room temperature for 30 min in the dark. Cell cycle distribution was determined by flow cytometric analysis of the DNA content using the BD FACS Aria II system (BD Biosciences). Data were analyzed by Modfit LT 4.0 (Verity Software House, Topsham, ME, USA).

Real-time PCR

Total RNA was extracted from NT2/D1 cells using TRIzol reagent (Life Technologies), and quantitative real-time reverse transcription (RT)-PCR was performed with QuantiTect SYBR Green RT-PCR Kit (QIAGEN, Valencia, CA, USA) using an ABI PRISM 7900HT sequence detection system (Applied Biosystems, Foster City, CA, USA) as previously reported (Hirata *et al.*, 2014). The relative change in transcript amounts was normalized to the expression levels of glyceraldehyde-3-phosphate dehydrogenase (GAPDH). The following primer sequences were used for real-time PCR analysis: human cdc25C: forward, 5′-AGGCAGCCTTGAGTTGCATAGAGA-3′, reverse, 5′-AGAGTTGGCTGGCTTGTGAGAAGA-3′;humancyclin B1:forward,5′-CGGGAAGTCACTGGAAACAT-3′,reverse, 5′-AAACATGGCAGTGACACCAA-3′; human GAPDH: forward, 5′-GTCTCCTCTGACTTCAACAGCG-3′, reverse, 5′-ACCACCCTGTTGCTGTAGCCAA-3′.

Western blot analysis

Western blot analysis was performed as previously reported (Kanda *et al.*, 2011). Briefly, cells were lysed with Cell Lysis Buffer (Cell Signaling Technology, Danvers, MA, USA). The proteins were then separated by sodium dodecyl sulfate-polyacrylamide gel electrophoresis (SDS-PAGE) and electrophoretically transferred to Immobilon-P membrane (Millipore, Billerica, MA, USA). The membranes were probed with an anti-cdc25C monoclonal antibody (1:1,000; Cell Signaling Technology), an anti-cyclin B1 monoclonal antibody (1:1,000; Cell Signaling Technology), and an anti-GAPDH polyclonal antibody (1:2,500; Abcam, Cambridge, UK) followed by incubation with horseradish peroxidase-conjugated secondary antibodies against rabbit or mouse IgG (Cel Signaling Technology). The bands were visualized using the ECL Western Blotting Analysis System (GE Healthcare, Buckinghamshire, UK), and images were acquired using a LAS-3000 Imager (FUJIFILM UK Ltd., Systems, Bedford, UK).

NAD-IDH activity assay

NAD-IDH activity was determined using the

Isocitrate Dehydrogenase Activity Colorimetric Assay Kit (Biovision, Mountain View, CA, USA), according to the manufacturer's instructions. Briefly, NT2/D1 cells were lysed in an assay buffer provided in the kit. The lysate was centrifuged at 14,000 *g* for 15 min, and the cleared supernatant was used for the assay.

NAD-IDHα knockdown

Knockdown studies were performed using NAD-IDHα shRNA lentiviruses from Sigma-Aldrich (MISSION shRNA) according to the manufacturer's protocol. A scrambled hairpin sequence was used as a negative control. Briefly, the cells were infected with the viruses at a multiplicity of infection of 10 in presence of 8 μg/mL hexadimethrine bromide (Sigma-Aldrich) for 24 hr, and were then subjected to selection with 0.5 μg/mL puromycin for 72 hr for further functional analyses.

Chemicals and reagents

Tributyltin Chloride was obtained from Tokyo Chemical Industry (Tokyo, Japan). Tin acetate (TA), apigenin, and dimethyl α-ketoglutarate (DMKG) were obtained from Sigma-Aldrich.

Statistical analysis

All data were presented as mean ± S.D. Analysis of variance (ANOVA) followed by post hoc Tukey's test was used to analyze the data in Figs. 1C, 1D, 1E, 2A, 2B, 3C, 4E, 5A, 5B, 6A and 6B. Student's t test was used to analyze the data in Figs. 3A, 3B, 4A, 4B and 4C. P-values less than 0.05 were considered to be statistically significant.

RESULTS

Effect of TBT on cell cycle progression

We have previously found that 100 nM TBT induced growth arrest in NT2/D1 cells (Yamada *et al.*, 2013). Here we investigated whether TBT affects cell cycle progression. Exposure to 100 nM TBT for 48 hr decreased the proportion of cells in the G1 phase (51.9% decrease) and increased of the proportion of cells in the G2/M phase (79.6% increase), compared with untreated control cells (Figs. 1A-E). In contrast, TBT did not affect the proportion of cells in the S phase. Moreover, exposure to tin acetate (TA), which is less toxic, did not affect cell cycle progression. These data suggest that TBT induces G2/M cell cycle arrest in the cells.

TBT exposure reduces G2/M cell cycle regulators, cdc25C and cyclin B1

To examine the molecular mechanism by which TBT induces G2/M cell cycle arrest, we assessed the protein levels of p53, a major cell cycle regulator. We found that p53 protein level was reduced after 24 hr of TBT treatment, whereas cisplatin, which is known to cause p53-dependent G2/M cell cycle arrest (Pani *et al.*, 2007), increased p53 levels (Supplementary Fig. 1). Since we could not observe p53-dependency in TBT-induced G2/M cell cycle arrest, we assessed cdc25C and its downstream factor, cyclin B1, which are also involved in G2/M progression of cell cycle. Western blot analysis revealed that cdc25C and cyclin B1 protein levels were reduced after 24 hr of TBT treatment (Fig. 2A). In contrast, exposure to TA did not affect cdc25C and cyclin B1 protein levels. Equal GAPDH protein expression levels were confirmed as a loading control. Next, we assessed the gene expression of cdc25C and cyclin B1. However, real-time PCR analysis showed that gene expression was not significantly altered by TBT exposure for both 24 and 48 hr (Fig. 2B). These data suggest that TBT-induced G2/M cell cycle arrest is caused by reduction of cdc25C and cyclin B1 proteins.

TBT induces G2/M cell cycle arrest via NAD-IDH

To investigate the molecular mechanisms by which cdc25C is degraded and G2/M cell cycle arrest is induced, we examined the effect of the PPARγ agonist rosiglitazone (RGZ), which is the genomic target of TBT. We found that RGZ did not induce G1 phase reduction and G2/M phase increase (Figs. 3A and B). RGZ at 100 nM induced PPARγ gene expression at similar level to 100 nM TBT in NT2/D1 cells (Fig. 3C), confirming the agonistic effect of RGZ on PPARγ expression described in previous report (Benkirane *et al.*, 2006). These data suggest that TBT induces G2/M cell cycle arrest in NT2/D1 cells through a non-genomic pathway. We next examined the involvement of the non-genomic target NAD-IDH. We used an NAD-IDH inhibitor apigenin (Arango *et al.*, 2013) at 10 μM, which reduced NAD-IDH activity to a level (22.4%) (Fig. 4A). As previously reported, 100 nM TBT had a similar inhibitory effect (24.4%; Yamada *et al.*, 2014). Treatment with apigenin (10 μM, 48 hr) decreased G1 phase ratio (58.6% decrease) and increased G2/M phase ratio (98.1% increase) (Figs. 4B and C). Similar to TBT, apigenin reduced protein expression of cdc25C and cyclin B1 without affecting gene expression (Figs. 4D and E). To further confirm the effect of apigenin, we performed knockdown (KD) experiments of NAD-IDHα, the catalytic subunit of NAD-IDH, using lentivirus-delivered shRNAs. Real-time PCR analysis showed that KD efficiency was approximately 40% (Yamada *et al.*, 2014). We could not obtain more highly KD cells because of cell

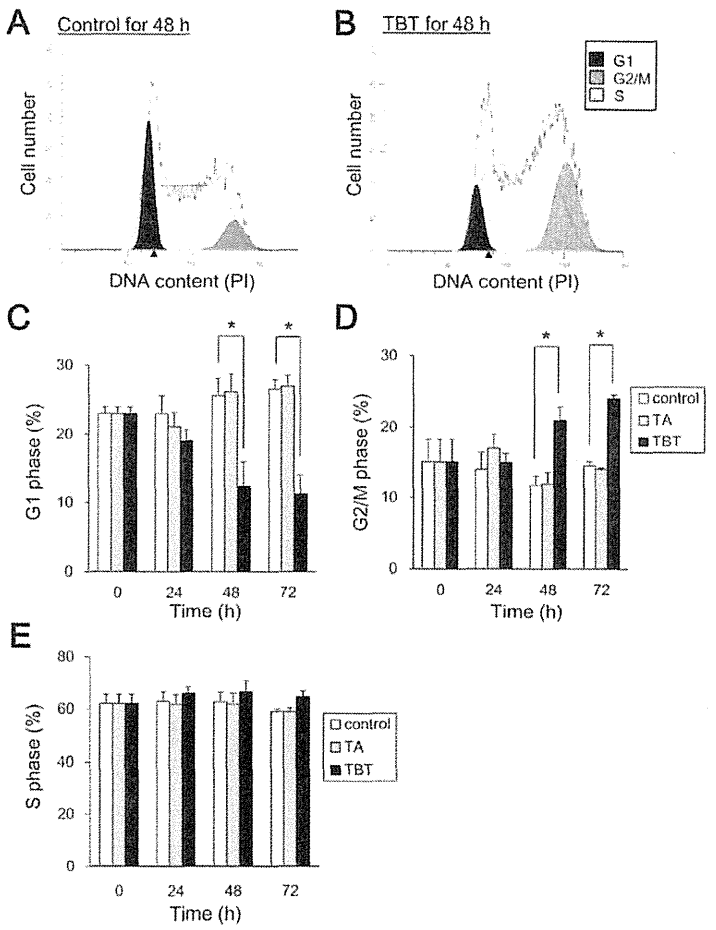

Fig. 1. Effect of TBT on cell cycle progression in NT2/D1 cells. Cells were exposed to 100 nM TA or TBT for 24, 48 or 72 hr. Cells were stained with propidium iodide (PI). Cell cycle distribution was determined by flow cytometric analysis of the DNA content on BD FACS Aria II. Representative cell cycle data in control (A) and TBT (B)-treated cells. The area ratio of G1 (C), G2/M (D) and S (E) phases was determined by Modfit LT 4.0. Data represent mean ± S.D. (n = 3). *P < 0.05.

death. Due to partial KD of the NAD-IDHα gene, NAD-IDH activity decreased by 22%, which is comparable to its decreased levels by TBT. In our previous studies, we observed that NAD-IDHα KD recovered the inhibitory effect of TBT on ATP content (Yamada *et al.*, 2014). This might be because the TBT target NAD-IDHα was already inhibited by shRNA and further inhibition by TBT was not observed in the knockdown cells. Similar to these data, NAD-IDHα KD abolished the TBT-induced G1 phase reduction and G2/M phase increase (Figs. 5A and B), suggesting the involvement of NAD-IDH on TBT effects. NAD-IDHα KD tended to decrease the proportion of cells in the G1 phase (24.1% ± 0.55 to 23.2% ± 0.34) and increase the proportion of cells in the G2/M phase (17.5% ± 1.6 to 20.3% ± 0.62), compared with control (Figs. 5A and B). Moreover, NAD-IDHα KD also abolished the TBT-induced reduction of cdc25C and cyclin B1 proteins (Fig. 5C). NAD-IDHα KD reduced the basal levels of cdc25C and cyclin B1 proteins, compared with control (Fig. 5C). These data suggest that NAD-IDH mediates TBT-induced G2/M cell cycle arrest in NT2/D1 cells. To further confirm the involvement of NAD-IDH, we treated the cells with dimethyl α-ketoglutarate (DMKG), a cell-permeable analog of α-ketoglutarate (Willenborg *et al.*, 2009). Incubation with DMKG prevented TBT-induced G2/M cell cycle arrest in NT2/D1 cells and

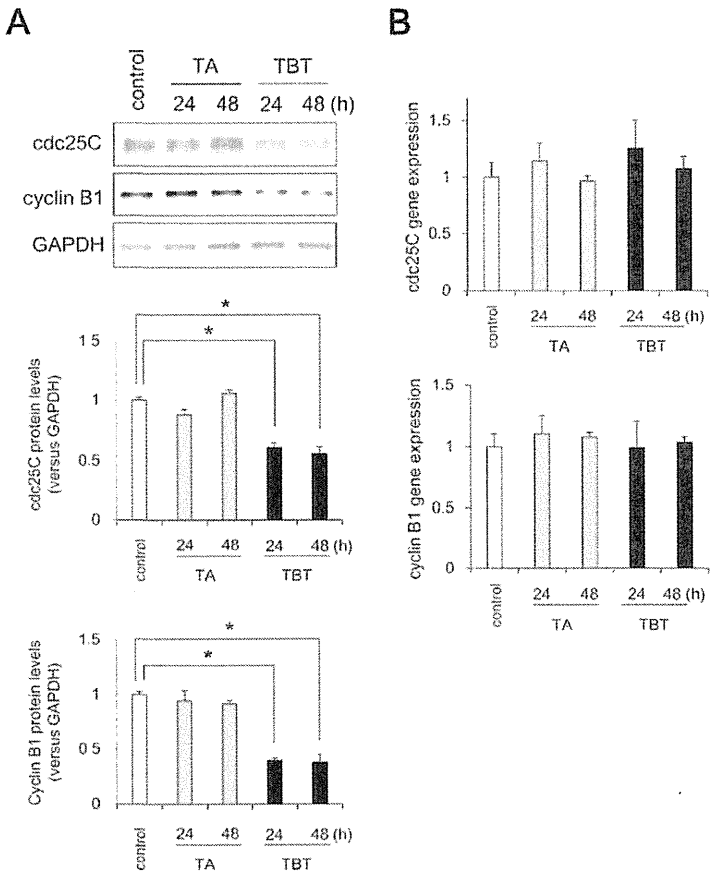

Fig. 2. Effect of TBT on expression levels of G2/M cell cycle regulators in NT2/D1 cells. After TBT exposure for 24 and 48 hr, protein expression was analyzed by western blot using anti-cdc25C, cyclin B1, or GAPDH antibodies (A). After TBT exposure for 24 or 48 hr, the expression of G2/M cell cycle regulators was analyzed by real time PCR (B). The gene expression was not significantly altered by TBT exposure. Data represent mean ± S.D. (n = 3).

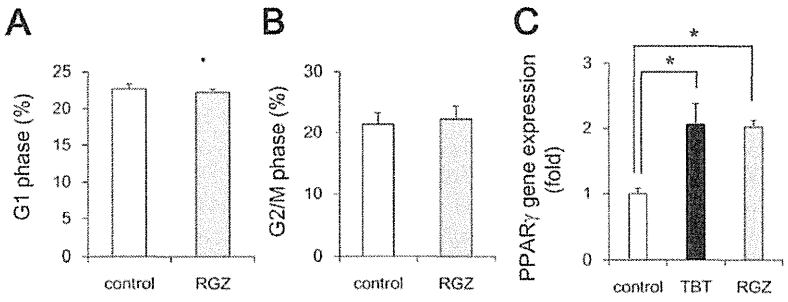

Fig. 3. Effect of RGZ on cell cycle progression in NT2/D1 cells. After RGZ exposure for 48 hr, cells were stained with propidium iodide (PI). The cell cycle distribution was determined by flow cytometric analysis of the DNA content using BD FACS Aria II. The ratio of G1 (A) and G2/M (B) phases was determined by Modfit LT 4.0. After exposure to TBT or RGZ, the expression of PPARγ was analyzed by real time PCR (C). The gene expression was comparably increased upon TBT or RGZ exposure. Data represent mean ± S.D. (n = 3). *P < 0.05.

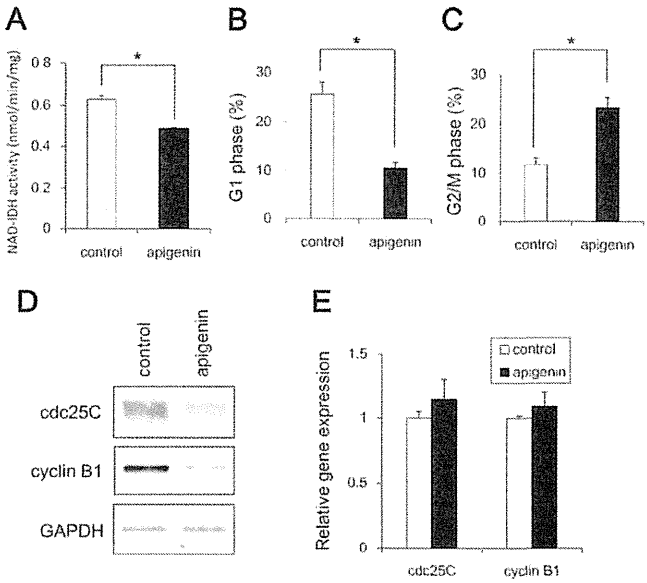

Fig. 4. Effect of apigenin on cell cycle progression in NT2/D1 cells. Cells were exposed to 10 μM apigenin for 24 hr and then determined NAD-IDH activity (A). Moreover, after exposure to apigenin for 48 hr, the cell cycle distribution was determined by flow cytometric analysis of the DNA content using BD FACS Aria II. The ratio of G1 (B) and G2/M (C) phases was determined by Modfit LT 4.0. The protein expressions in the cell lysate were analyzed by western blot using anti-cdc25C, cyclin B1, or GAPDH antibodies (D). The expression of G2/M cell cycle regulators was analyzed by real time PCR (E). The gene expression was not significantly altered upon apigenin exposure. Data represent mean ± S.D. (n = 3). *P < 0.05.

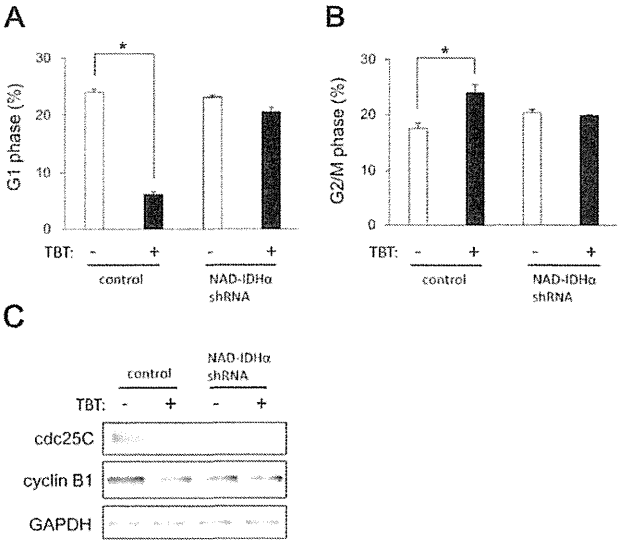

Fig. 5. Effect of NAD-IDH knockdown on cell cycle progression in NT2/D1 cells. Cells were infected with lentiviruses to express a shRNA against NAD-IDHα or a scrambled sequence shRNA (control). The infected cells were subjected to selection with 0.5 μg/mL puromycin for 72 hr and were then exposed to TBT at 100 nM for 48 hr. After staining with PI, cell cycle distribution was determined by flow cytometric analysis of the DNA content using BD FACS Aria II. The ratio of G1 (A) and G2/M (B) phases was analyzed by Modfit LT 4.0. The protein expressions in cell lysates were analyzed by western blot using anti-cdc25C, cyclin B1, or GAPDH antibodies (C). Data represent mean ± S.D. (n = 3). *P < 0.05.

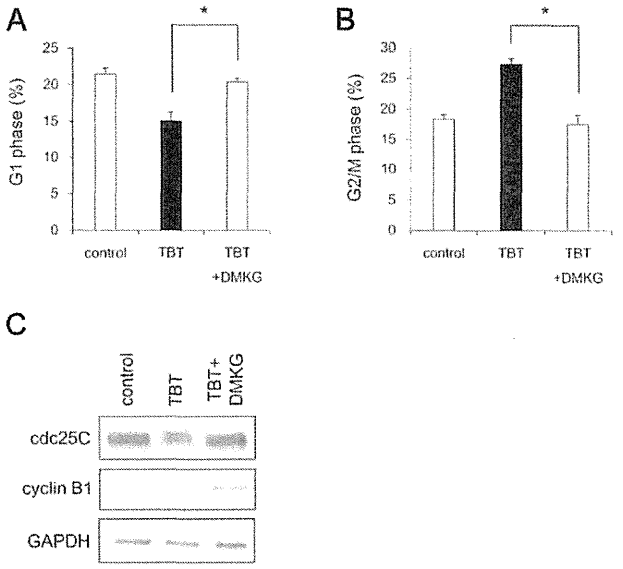

Fig. 6. Effect of dimethyl α-ketoglutarate (DMKG) on TBT-induced G2/M cell cycle arrest in NT2/D1 cells. Cells were exposed to 100 nM TBT and 7 mM DMKG for 48 hr. Cells were then stained with propidium iodide (PI) and cell cycle distribution was determined by flow cytometric analysis of the DNA content using BD FACS Aria II. The ratio of G1 (A) and G2/M (B) phases was analyzed by Modfit LT 4.0. Next, the protein expressions in cell lysates were analyzed by western blot using anti-cdc25C, cyclin B1, or GAPDH antibodies (C). Data represent mean ± S.D. (n = 3). *P < 0.05.

recovered the ratio of G1 and G2/M phases to the basal level (Figs. 6A and B). DMKG treatment also recovered TBT-induced protein reduction of cdc25C and cyclin B1 (Fig. 6C). Taken together, these data suggest that NAD-IDH mediates TBT-induced G2/M cell cycle arrest via cdc25C reduction in NT2/D1 cells.

DISCUSSION

Our data suggest that nanomolar TBT levels induce G2/M cell cycle arrest through the protein reduction of cdc25C and thereafter cyclin B1 (Figs. 1 and 2). Since the protein expression of p53 is decreased after TBT exposure, TBT-induced G2/M cell cycle arrest seems to be p53 independent. Consistent with our data, recent study has reported that nearly micromolar TBT levels induce G2/M cell cycle arrest in human amniotic cells via protein phosphatase (PP) 2A inhibition-mediated extracellular-signal-regulated kinase (ERK) inactivation (Zhang *et al.*, 2014). Since we did not observe the reduction of phospho-ERK in NT2/D1 cells after nanomolar levels of TBT exposure (data not shown), the mechanism of inducing G2 arrest may differ depending on the TBT levels and cell type. Moreover, several chemical stressors have been reported to cause G2/M cell cycle arrest through the protein reduction of cell cycle regulators (Chaudhary *et al.*, 2013; Nam *et al.*, 2010; Ouyang *et al.*, 2009). For instance, 4-Hydroxynonenal, an inducer of oxidative stress, causes DNA damage and induces G2/M cell cycle arrest in hepatocellular carcinoma HepG2 and Hep3B cells, following reduction of cdc25C and thereafter cyclin B1 proteins in a p53-independent manner (Chaudhary *et al.*, 2013). Reduction of cdc25C protein may be mediated by the ubiquitin-proteasome system in NT2/D1 cells. Cdc25C has been reported to be degraded via ubiquitination by BRCA1 during G2/M cell cycle arrest in breast cancer cell lines (Shabbeer *et al.*, 2013). During G2/M cell cycle arrest, another cell cycle regulators, such as Plk1, cdc25A and CDK1, are also known to be degraded by ubiquitin ligases, such as multi-subunit E3 ubiquitin ligases, Skp1-Cullin1-F-box Complex (SCF) or Anaphase Promoting Complex (APC) (Bassermann and Pagano, 2010). Further studies should determine whether ubiquitin ligases are involved in TBT-induced cdc25C reduction and subsequent G2/M cell cycle arrest in embryonic cells.

Our data using apigenin showed that TBT-induced G2/M cell cycle arrest is caused by NAD-IDH inhibition

(Fig. 4) and the data were verified by NAD-IDH knockdown and DMKG experiments (Figs. 5, 6). We used apigenin as a NAD-IDH inhibitor. We also confirmed the data by knockdown experiments. Since Apigenin has been reported to inhibit not only NAD-IDH but also hnRNPA2 and NF-κB (Arango *et al.*, 2013), we can not rule out the possibility that apigenin-induced G2/M cell cycle arrest was induced by other targets. Our previous report indicates that TBT induces mitochondrial dysfunction, such as impaired mitochondrial morphological dynamics and reduced ATP production via NAD-IDH in embryonic carcinoma cells (Yamada *et al.*, 2015). Considering that NAD-IDH is a mitochondrial enzyme, TBT-induced G2/M cell cycle arrest is caused by mitochondrial dysfunction through NAD-IDH inhibition. NAD-IDH catalyzes the reduction of NAD to NADH, which is oxidized by the electron transport chain and is required to generate proton electrochemical gradients across the inner mitochondrial membrane (Saraste, 1999). Thus, inhibition of NAD-IDH by TBT may reduce the NADH supply, thereby dissipating the proton electrochemical gradient. Intracellular Ca^{2+} may be also involved in mitochondrial dysfunction. Previous reports have shown that several anticancer drugs induce G2/M cell cycle arrest and apoptosis by depolarizing mitochondrial membrane potential and increasing intracellular Ca^{2+} (Fang *et al.*, 2014; Guo *et al.*, 2014). With respect to intracellular Ca^{2+}, there has been also reported that TBT induces mobilization of Ca^{2+} from intracellular stores and results in phosphorylation of MAPKs because its suppression by chelation of intracellular Ca^{2+} in human T lymphoblastoid cells (Yu *et al.*, 2000). Thus, Ca^{2+} release from depolarized mitochondria may induce G2/M cell cycle arrest after TBT exposure. Further studies should determine how the downstream signaling of NAD-IDH induces reduction of the cdc25C protein and subsequent G2/M cell cycle arrest after TBT exposure in embryonic cells.

In our previous studies, we have observed that TBT degrades mitofusin proteins and induces mitochondrial fission via the NAD-IDH inhibition. Moreover, we have also shown that TBT results in growth arrest by targeting the glycolytic systems (Yamada *et al.*, 2014). Both mitochondrial fission and glycolysis have been reported to be linked to cell cycle alterations (Yamamori *et al.*, 2015; Zhai *et al.*, 2013). Thus, we are currently investigating whether TBT-induced mitochondrial fission or glycolytic inhibition are linked to G2/M cell cycle arrest or not.

In summary, we demonstrate that TBT mediates G2/M cell cycle arrest through inhibition of NAD-IDH, representing a novel non-genomic pathway of TBT-induced toxicity (Fig. 7). These negative effects of TBT on the cell cycle could result in direct inhibition of cell growth. Thus, TBT-induced G2/M cell cycle arrest via NAD-IDH in embryonic cells may represent a novel mechanism of cytotoxicity associated with nanomolar level exposure of EDCs.

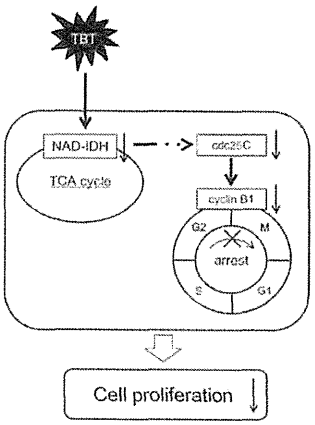

Fig. 7. Proposed model of TBT toxicity through non-genomic pathways in human embryonic carcinoma cells. Nanomolar TBT levels inhibit NAD-IDH activity. TBT induces G2/M cell cycle arrest via the protein reduction of cdc25C and its downstream target, cyclin B1. This TBT-induced G2/M cell cycle arrest may mediate cell growth inhibition.

ACKNOWLEDGMENTS

This work was supported by a Health and Labour Sciences Research Grant from the Ministry of Health, Labour and Welfare, Japan (#H25-Kagaku-Ippan-002 to Y. Kanda), a Grant-in-Aid for Scientific Research from the Ministry of Education, Culture, Sports, Science, and Technology, Japan (#26293056, #26670041 to Y. Kanda), the Research on Regulatory Harmonization and Evaluation of Pharmaceuticals, Medical Devices, Regenerative and Cellular Therapy Products, Gene Therapy Products, and Cosmetics from Japan Agency for Medical Research and development, AMED (To Y. Sekino), and a grant from the Smoking Research Foundation (Y. Kanda).

Conflict of interest---- The authors declare that there is no conflict of interest.

REFERENCES

Arango, D., Morohashi, K., Yilmaz, A., Kuramochi, K., Parihar, A., Brahimaj, B., Grotewold, E. and Doseff, A.I. (2013): Molecular basis for the action of a dietary flavonoid revealed by the com-

prehensive identification of apigenin human targets. Proc. Natl. Acad. Sci. USA, **110**, E2153-E2162.

Bassermann, F. and Pagano, M. (2010): Dissecting the role of ubiquitylation in the DNA damage response checkpoint in G2. Cell Death Differ., **17**, 78-85.

Benkirane, K., Amiri, F., Diep, Q.N., El Mabrouk, M. and Schiffrin, E.L. (2006): PPAR-gamma inhibits ANG II-induced cell growth via SHIP2 and 4E-BP1. Am. J. Physiol. Heart Circ. Physiol., **290**, H390-H397.

Chaudhary, P., Sharma, R., Sahu, M., Vishwanatha, J.K., Awasthi, S. and Awasthi, Y.C. (2013): 4-Hydroxynonenal induces G2/M phase cell cycle arrest by activation of the ataxia telangiectasia mutated and Rad3-related protein (ATR)/checkpoint kinase 1 (Chk1) signaling pathway. J. Biol. Chem., **288**, 20532-20546.

Donzelli, M. and Draetta, G.F. (2003): Regulating mammalian checkpoints through Cdc25 inactivation. EMBO Rep., **4**, 671-677.

Dopp, E., Hartmann, L.M., Florea, A.M., Rettenmeier, A.W. and Hirner, A.V. (2004): Environmental distribution, analysis, and toxicity of organometal(loid) compounds. Crit. Rev. Toxicol., **34**, 301-333.

Fang, C., Zhang, J., Qi, D., Fan, X., Luo, J., Liu, L. and Tan, Q. (2014): Evodiamine induces G2/M arrest and apoptosis via mitochondrial and endoplasmic reticulum pathways in H446 and H1688 human small-cell lung cancer cells. PLoS One, **9**, e115204.

Gabrielli, B., Brooks, K. and Pavey, S. (2012): Defective cell cycle checkpoints as targets for anti-cancer therapies. Front. Pharmacol., **3**, 9.

Gärdlund, A.T., Archer, T., Danielsen, K., Danielsson, B., Frederiksson, A., Lindquist, N.G., Lindström, H. and Luthman, J. (1991): Effects of prenatal exposure to tributyltin and trihexyltin on behaviour in rats. Neurotoxicol. Teratol., **13**, 99-105.

Guo, J., Zhao, W., Hao, W., Ren, G., Lu, J. and Chen, X. (2014): Cucurbitacin B induces DNA damage, G2/M phase arrest, and apoptosis mediated by reactive oxygen species (ROS) in leukemia K562 cells. Anticancer Agents Med. Chem., **14**, 1146-1153.

Hirata, N., Yamada, S., Shoda, T., Kurihara, M., Sekino, Y. and Kanda, Y. (2014): Sphingosine-1-phosphate promotes expansion of cancer stem cells via S1PR3 by a ligand-independent Notch activation. Nat. Commun., **5**, 4806.

Kanayama, T., Kobayashi, N., Mamiya, S., Nakanishi, T. and Nishikawa, J. (2005): Organotin compounds promote adipocyte differentiation as agonists of the peroxisome proliferator-activated receptor gamma/retinoid X receptor pathway. Mol. Pharmacol., **67**, 766-774.

Kanda, Y., Hinata, T., Kang, S.W. and Watanabe, Y. (2011): Reactive oxygen species mediate adipocyte differentiation in mesenchymal stem cells. Life Sci., **89**, 250-258.

Kawabe, T. (2004): G2 checkpoint abrogators as anticancer drugs. Mol. Cancer Ther., **3**, 513-519.

Mitra, S., Gera, R., Siddiqui, W.A. and Khandelwal, S. (2013): Tributyltin induces oxidative damage, inflammation and apoptosis via disturbance in blood–brain barrier and metal homeostasis in cerebral cortex of rat brain: an *in vivo* and *in vitro* study. Toxicology, **310**, 39-52.

Nakatsu, Y., Kotake, Y., Takai, N. and Ohta, S. (2010): Involvement of autophagy via mammalian target of rapamycin (mTOR) inhibition in tributyltin-induced neuronal cell death. J. Toxicol. Sci., **35**, 245-251.

Nam, C., Doi, K. and Nakayama, H. (2010): Etoposide induces G2/M arrest and apoptosis in neural progenitor cells via DNA damage and an ATM/p53-related pathway. Histol. Histopathol., **25**, 485-493.

Ouyang, G., Yao, L., Ruan, K., Song, G., Mao, Y. and Bao, S. (2009): Genistein induces G2/M cell cycle arrest and apoptosis of human ovarian cancer cells via activation of DNA damage checkpoint pathways. Cell Biol. Int., **33**, 1237-1244.

Pani, E., Stojic, L., El-Shemerly, M., Jiricny, J. and Ferrari, S. (2007): Mismatch repair status and the response of human cells to cisplatin. Cell Cycle, **6**, 1796-1802.

Saraste, M. (1999): Oxidative phosphorylation at the fin de siècle. Science, **283**, 1488-1493.

Shabbeer, S., Omer, D., Berneman, D., Weitzman, O., Alpaugh, A., Pietraszkiewicz, A., Metsuyanim, S., Shainskaya, A., Papa, M.Z. and Yarden, R.I. (2013): BRCA1 targets G2/M cell cycle proteins for ubiquitination and proteasomal degradation. Oncogene, **32**, 5005-5016.

Shackelford, R.E., Kaufmann, W.K. and Paules, R.S. (1999): Cell cycle control, checkpoint mechanisms, and genotoxic stress. Environ. Health Perspect., **107**, 5-24.

Whalen, M.M., Loganathan, B.G. and Kannan, K. (1999): Immunotoxicity of environmentally relevant concentrations of butyltins on human natural killer cells *in vitro*. Environ. Res., **81**, 108-116.

Willenborg, M., Panten, U. and Rustenbeck, I. (2009): Triggering and amplification of insulin secretion by dimethyl alpha-ketoglutarate, a membrane permeable alpha-ketoglutarate analogue. Eur. J. Pharmacol., **607**, 41-46.

Yamada, S., Kotake, Y., Sekino, Y. and Kanda, Y. (2013): AMP-activated protein kinase-mediated glucose transport as a novel target of tributyltin in human embryonic carcinoma cells. Metallomics, **5**, 484-491.

Yamada, S., Kotake, Y., Demizu, Y., Kurihara, M., Sekino, Y. and Kanda, Y. (2014): NAD-dependent isocitrate dehydrogenase as a novel target of tributyltin in human embryonic carcinoma cells. Sci. Rep., **4**, 5952.

Yamada, S., Kotake, Y., Nakano, M., Sekino, Y. and Kanda, Y. (2015): Tributyltin induces mitochondrial fission through NAD-IDH dependent mitofusin degradation in human embryonic carcinoma cells. Metallomics, **7**, 1240-1246.

Yamamori, T., Ike, S., Bo, T., Sasagawa, T., Sakai, Y., Suzuki, M., Yamamoto, K., Nagane, M., Yasui, H. and Inanami, O. (2015): Inhibition of the mitochondrial fission protein dynamin-related protein 1 (Drp1) impairs mitochondrial fission and mitotic catastrophe after X-irradiation. Mol. Biol. Cell, **26**, 4607-4617.

Yu, L., Zhang, X., Yuan, J., Cao, Q., Liu, J., Zhu, P. and Shi, H. (2011): Teratogenic effects of triphenyltin on embryos of amphibian (*Xenopus tropicalis*): a phenotypic comparison with the retinoid X and retinoic acid receptor ligands. J. Hazard Mater., **192**, 1860-1868.

Yu, Z.P., Matsuoka, M., Wispriyono, B., Iryo, Y. and Igisu, H. (2000): Activation of mitogen-activated protein kinases by tributyltin in CCRF-CEM cells: role of intracellular Ca(2+). Toxicol. Appl. Pharmacol., **168**, 200-207.

Zhai, X., Yang, Y., Wan, J., Zhu, R. and Wu, Y. (2013): Inhibition of LDH-A by oxamate induces G2/M arrest, apoptosis and increases radiosensitivity in nasopharyngeal carcinoma cells. Oncol. Rep., **30**, 2983-2991.

Zhang, Y., Go, Z. and Xu, L. (2014): Tributyltin induces a G2/M cell cycle arrest in human amniotic cells via PP2A inhibition-mediated inactivation of the ERK1/2 cascades. Environ. Toxicol. Pharmacol., **37**, 812-818.

Biochemical and Biophysical Research Communications 470 (2016) 300–305

Contents lists available at ScienceDirect

Biochemical and Biophysical Research Communications

journal homepage: www.elsevier.com/locate/ybbrc

Nicotine induces mitochondrial fission through mitofusin degradation in human multipotent embryonic carcinoma cells

Naoya Hirata [a, 1], Shigeru Yamada [a, 1], Miki Asanagi [a, b], Yuko Sekino [a], Yasunari Kanda [a, *]

[a] Division of Pharmacology, National Institute of Health Sciences, Japan
[b] Faculty of Engineering, Department of Materials Science and Engineering, Yokohama National University, Japan

ARTICLE INFO

Article history:
Received 5 January 2016
Accepted 10 January 2016
Available online 13 January 2016

Keywords:
Embryonic cells
Cigarette smoking
Nicotine
Mitochondrial fission
Mitofusin

ABSTRACT

Nicotine is considered to contribute to the health risks associated with cigarette smoking. Nicotine exerts its cellular functions by acting on nicotinic acetylcholine receptors (nAChRs), and adversely affects normal embryonic development. However, nicotine toxicity has not been elucidated in human embryonic stage. In the present study, we examined the cytotoxic effects of nicotine in human multipotent embryonal carcinoma cell line NT2/D1. We found that exposure to 10 μM nicotine decreased intracellular ATP levels and inhibited proliferation of NT2/D1 cells. Because nicotine suppressed energy production, which is a critical mitochondrial function, we further assessed the effects of nicotine on mitochondrial dynamics. Staining with MitoTracker revealed that 10 μM nicotine induced mitochondrial fragmentation. The levels of the mitochondrial fusion proteins, mitofusins 1 and 2, were also reduced in cells exposed to nicotine. These nicotine effects were blocked by treatment with mecamylamine, a nonselective nAChR antagonist. These data suggest that nicotine degrades mitofusin in NT2/D1 cells and thus induces mitochondrial dysfunction and cell growth inhibition in a nAChR-dependent manner. Thus, mitochondrial function in embryonic cells could be used to assess the developmental toxicity of chemicals.

1. Introduction

Growing evidence suggest that maternal smoking during pregnancy is related to adverse neurodevelopmental outcomes in the offspring, including lower intelligence quotients and deficits in learning and memory [1,2]. Nicotine is a naturally occurring alkaloid that is present in tobacco leaves and is considered to contribute to the negative effects of cigarette smoking on health [2,3]. Nicotine exerts its cellular functions by activating nicotinic acetylcholine receptors (nAChRs), which are heterodimers composed of combinations of different types of α subunit (α1–α10) and β subunit (β1–β4) [4]. α8-nAChR has not been identified in human. Recent studies have shown that nAChRs are present in a variety of cells, such as cancer cells, vascular smooth muscle, and neural cells [3–6]. Activation of nAChRs by nicotine promotes the release of various neurotransmitters (including dopamine, norepinephrine, acetylcholine, glutamate) [7]. Altered regulation of neurotransmitter levels can adversely affect key events in normal brain development, such as the formation of neural circuits and neurotransmitter systems [7,8]. Therefore, it is necessary to elucidate the cytotoxic effects of nicotine on embryonic development.

Nicotine toxicity has been reported to affect mitochondrial function both *in vitro* and *in vivo*. For example, nicotine exposure alters mitochondrial membrane potential (MMP), increases an oxidative stress, and induces apoptosis in colon adenocarcinoma HCT-116 cell [9]. Another study has shown that nicotine exposure reduced the activity of an enzyme in the pancreatic mitochondrial respiratory chain, and impaired glucose-stimulated insulin secretion in neonatal rats [10]. However, the precise mechanisms underlying the effects of nicotine on mitochondrial function remain largely unknown.

Growing evidence suggest that mitochondria undergo continuous morphological dynamics involving fusion and fission cycles. These dynamics play a key role in maintenance of normal mitochondrial functions, such as ATP production [11]. Mitochondrial fusion and fission are regulated by several GTPases. Mitofusin 1 and 2 (Mfn1, 2) and optic atrophy 1 (Opa1) induce fusion of the outer and inner mitochondrial membranes, respectively [12,13]. In contrast, dynamin-related protein 1 (Drp1) is a cytoplasmic protein that assembles into rings surrounding the outer mitochondrial

* Corresponding author. 1-18-1, Kamiyoga, Setagaya-ku, 158-8501, Japan.
E-mail address: kanda@nihs.go.jp (Y. Kanda).
[1] Equally contributed.

http://dx.doi.org/10.1016/j.bbrc.2016.01.063
0006-291X/

membrane, where it interacts with fission protein 1 (Fis1) to promote fission [14,15]. For example, pigment epithelium-derived factor is reported to improve mitochondrial function by stabilizing mitochondrial fusion in retinal pigment epithelial cells [16]. In contrast, the anti-tumor agent, doxorubicin, facilitates mitochondrial fragmentation and apoptosis by promoting Mfn2 degradation in sarcoma U2OS cells [17].

In the present study, we hypothesized a possible link between nicotine toxicity and mitochondrial function in human mulitpotent NT2/D1 cells, which have neural differentiation capability. Our results showed that exposure to 10 μM nicotine decreased intracellular ATP levels and inhibited cell growth. Moreover, nicotine exposure induced Mfn degradation and mitochondrial fragmentation via nicotinic acetylcholine receptors (nAChRs). Thus, nicotine induces toxicity through impairment of mitochondrial quality control in human NT2/D1 cells.

2. Materials and methods

2.1. Cell culture

The human multipotent embryonal carcinoma NT2/D1 cells were obtained from the American Type Culture Collection (Manassas, VA, USA). SH-SY5Y cells were obtained from European Collection of Animal Cell Culture (Salisbury, Wiltshire, UK). The cells were cultured in Dulbecco's modified Eagle's medium (DMEM; Sigma–Aldrich, St. Louis, MO, USA) supplemented with 10% fetal bovine serum (FBS; Biological Industries, Ashrat, Israel) and 0.05 mg/ml penicillin-streptomycin mixture (Life Technologies, Carlsbad, CA, USA) at 37 °C in the presence of 5% CO_2.

2.2. Cell proliferation assay

Cell viability was measured using the CellTiter 96 AQueous One Solution Cell Proliferation Assay (Promega, Madison, WI, USA), as previously described [18]. Briefly, NT2/D1 cells were seeded into 96-well plate and exposed to different concentrations of nicotine. After exposure to nicotine, One Solution Reagent was added to each well, and the plate was incubated at 37 °C for another 2 h. Absorbance was measured at 490 nm by iMark microplate reader (Bio-Rad, Hercules, CA, USA).

2.3. Measurement of intracellular ATP levels

The intracellular ATP content was measured using the ATP Determination Kit (Life Technologies), as previously described [19]. Briefly, the cells were washed and lysed with phosphate-buffered saline containing 0.1% Triton X-100. The resulting cell lysates were added to a reaction mixture containing 0.5 mM D-luciferin, 1 mM dithiothreitol, and 1.25 μg/ml luciferase and incubated for 30 min at room temperature. Luminescence was measured using a Wallac1420ARVO fluoroscan (Perkin–Elmer, Waltham, MA, USA). The luminescence intensities were normalized to the total protein content.

2.4. Assessment of mitochondrial fusion

After treatment with nicotine (10 μM, 24 h), cells were fixed with 4% paraformaldehyde and stained with 50 nM MitoTracker Red CMXRos (Cell Signaling Technology, Danvers, MA, USA) and 0.1 μg/ml 4′,6-diamidino-2-phenylindole (DAPI; Dojin, Kumamoto, Japan). Changes in mitochondrial morphology were observed using a confocal laser microscope (Nikon A1). Images (n = 3–7) of random fields were taken, and the number of cells displaying mitochondrial fusion (<10% punctiform) was counted in each image, as previously described [20]. The number of cells showing mitochondrial fission was calculated by subtracting the number of cells with mitochondrial fusion from the total cell number.

2.5. Real-time PCR

Total RNA was isolated from NT2/D1 cells using TRIzol reagent (Life Technologies), and quantitative real-time reverse transcription (RT)-PCR with QuantiTect SYBR Green RT-PCR Kit (QIAGEN, Valencia, CA, USA) was performed using an ABI PRISM 7900HT sequence detection system (Applied Biosystems, Foster City, CA, USA) as previously described [21]. The relative change in the amount of transcript was normalized to the mRNA levels of glyceraldehyde-3-phosphate dehydrogenase (GAPDH). The following primer sequences were used for real-time PCR analysis: *nAChRα1*, forward, 5′-CTGGACCTACGACGGCTCT-3′ and reverse, 5′-CGCTGCATGACGAAGTGGT-3′; *nAChRα2*, forward, 5′-ACACTTCAGACGTGGTGATTG-3′ and reverse, 5′-CCACTCCTGTTTTAGCCAGAC-3′; *nAChRα3*, forward, 5′-ACCTGTGGCTCAAGCAAATCT-3′ and reverse, 5′-GCAGGGACACGCATGAACT-3′; *nAChRα4*, forward, 5′-GGAGGGCGTCCAGTACATTG-3′ and reverse, 5′-GAAGATGCGGTCGATGACCA-3′; *nAChRα5*, forward, 5′-AGATGGAACCCTGATGACTATGGT-3′ and reverse, 5′-AAACGTCCATCTGCATTATCAAAC-3′; *nAChRα6*, forward, 5′-GGCAGGGATTCCTTCATGGG-3′ and reverse, 5′-GCCTCTCCTCAGTTGCACAG-3′; *nAChRα7*, forward, 5′-CATGGCCTTCTCGGTCTTCA-3′ and reverse, 5′-CACGGCCTCCACGAAGTT-3′; *nAChRα10*, forward, 5′-CAGATGCCTACCTACGATGGG-3′ and reverse, 5′-GGGAAGGCTGCTACATCCA-3′; *nAChRβ1*, forward, 5′-TGAGACCTCACTATCAGTACCCA-3′ and reverse, 5′-AGAACCACGACACTAAGGATGA-3′; *nAChRβ2*, forward, 5′-GGTGACAGTACAGCTTATGGTG-3′ and reverse, 5′-AGGCGATAATCTTCCCACTCC-3′; *nAChRβ3*, forward, 5′-TGCTGGTTCTCATCGTCCTTG-3′ and reverse, 5′-GCATCTTCATTTTCGGCGATTGA-3′; *nAChRβ4*, forward, 5′-CAGCTTATCAGCGTGAATGAGC-3′ and reverse, 5′-GTCAGGCGGTAATCAGTCCAT-3′; *Drp1*, forward, 5′-TGGGCGCCGACATCA-3′ and reverse, 5′-GCTCTGCGTTCCCACTACGA-3′; *Fis1*, forward, 5′-TACGTCCGCGGGTTGCT-3′ and reverse, 5′-CCAGTTCCTTGGCCTGGTT-3′; *Mfn1*, forward, 5′-GGCATCTGTGGCCGAGTT-3′ and reverse, 5′-ATTATGCTAAGTCTCCGCTCCAA-3′; *Mfn2*, forward, 5′-GCTCGGAGGCACATGAAAGT-3′ and reverse, 5′-ATCACGGTGCTCTTCCCATT-3′; *Opa1*, forward, 5′-GTGCTGCCCGCCTAGAAA-3′ and reverse, 5′-TGACAGGCACCCGTACTCAGT-3′; *GAPDH*, forward, 5′-GTCTCCTCTGACTTCAACAGCG-3′ and reverse, 5′-ACCACCCTGTTGCTGTAGCCAA-3′.

2.6. Western blot analysis

Western blot analysis was performed as previously reported [22]. Briefly, the cells were lysed with Cell Lysis Buffer (Cell Signaling Technology). The proteins were then separated by sodium dodecyl sulfate-polyacrylamide gel electrophoresis (SDS-PAGE) and electrophoretically transferred to Immobilon-P (Millipore, Billerica, MA, USA). The membranes were probed with anti-Drp1 monoclonal antibodies (1:1000; Cell Signaling Technology), anti-Fis1 polyclonal antibodies (1:200; Santa Cruz Biotechnology, Santa Cruz, CA, USA), anti-Mfn1 polyclonal antibodies (1:1000; Cell Signaling Technology), anti-Mfn2 monoclonal antibodies (1:1000; Cell Signaling Technology), anti-Opa1 monoclonal antibodies (1:1000; BD Biosciences), and anti-β-actin monoclonal antibodies (1:5000; Sigma–Aldrich). The membranes were then incubated with secondary antibodies against rabbit or mouse IgG conjugated to horseradish peroxidase (Cell Signaling Technology). The bands were visualized using the ECL Western Blotting Analysis System (GE

Healthcare, Buckinghamshire, UK), and images were acquired using a LAS-3000 Imager (FUJIFILM UK Ltd., Systems, Bedford, UK).

2.7. Chemicals and reagents

Nicotine was obtained from Wako Pure Chemicals (Osaka, Japan). Mecamylamine hydrochloride (MCA) and m-chlorophenylhydrazone (CCCP) were obtained from Sigma–Aldrich.

2.8. Statistical analysis

All data were presented as means ± S.D. ANOVA followed by post hoc Fisher test was used to analyze data in Fig. 1A and B and Figs. 2–4C. Student's *t*-test was used to analyze data in Fig. 4A. *P*-values less than 0.05 were considered to be statistically significant.

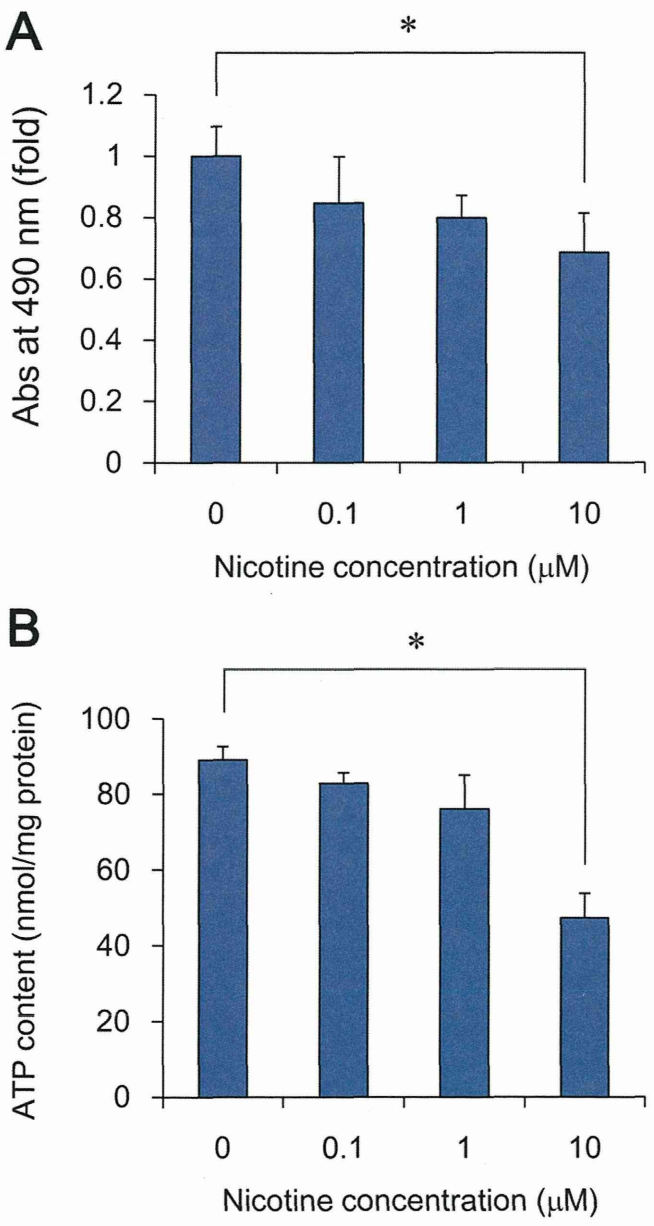

Fig. 1. Nicotine inhibits cell proliferation via intracellular ATP decrease in NT2/D1 cells. A. Cells were exposed to different concentrations of nicotine for 72 h. Cell viability was examined using the CellTiter 96 AQueous One Solution Cell Proliferation Assay. B. After treatment with different concentrations of nicotine for 24 h, intracellular ATP content was determined in cell lysates. Data represent the mean ± SD (n = 3). *P < 0.05.

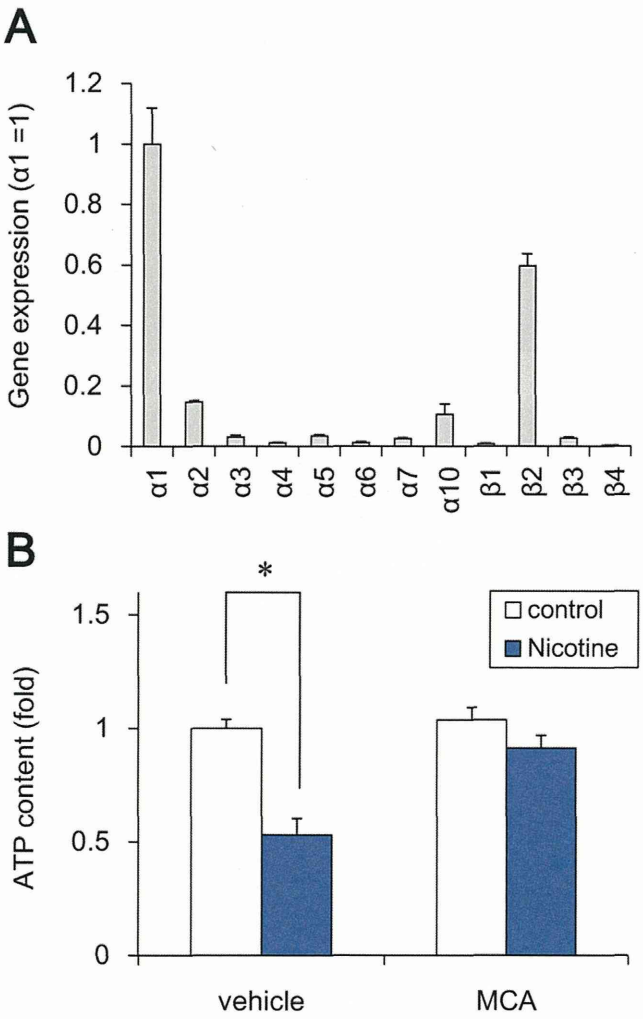

Fig. 2. Nicotine reduces intracellular ATP levels via nAChRs in NT2/D1 cells. A. Expression of AChR subtypes was analyzed by real-time PCR in NT2/D1 cells. The relative changes were determined by normalizing with GAPDH. B. After treatment with 10 μM nicotine and/or 30 μM MCA for 24 h, intracellular ATP content was determined in cell lysates. Data represent the mean ± SD (n = 3). *P < 0.05.

3. Results

3.1. Cytotoxic effects of nicotine in NT2/D1 cells

To examine the effects of nicotine on human multipotent embryonic cells, we exposed the cells to different concentrations of nicotine for 72 h and measured cell viability by MTT assay using human multipotent embryonic carcinoma NT2/D1 cells, which have an ability to differentiate into neuronal cells. We found that treatment with 10 μM nicotine significantly inhibited cell proliferation (Fig. 1A). Similarly, exposure to 10 μM nicotine significantly reduced the ATP content of the cells (Fig. 1B). To further investigate whether the nicotine effects are selective for undifferentiated cells, we used human SH-SY5Y neuroblastoma cells. We found that exposure to 10 μM nicotine had little effect on proliferation and ATP content of SH-SY5Y cells (Fig. S1).

We next examined the nAChR mRNA levels by real-time PCR and confirmed that nAChR subtypes except α9-nAChR were expressed in NT2/D1 cells (Fig. 2A). To examine whether the inhibition of ATP

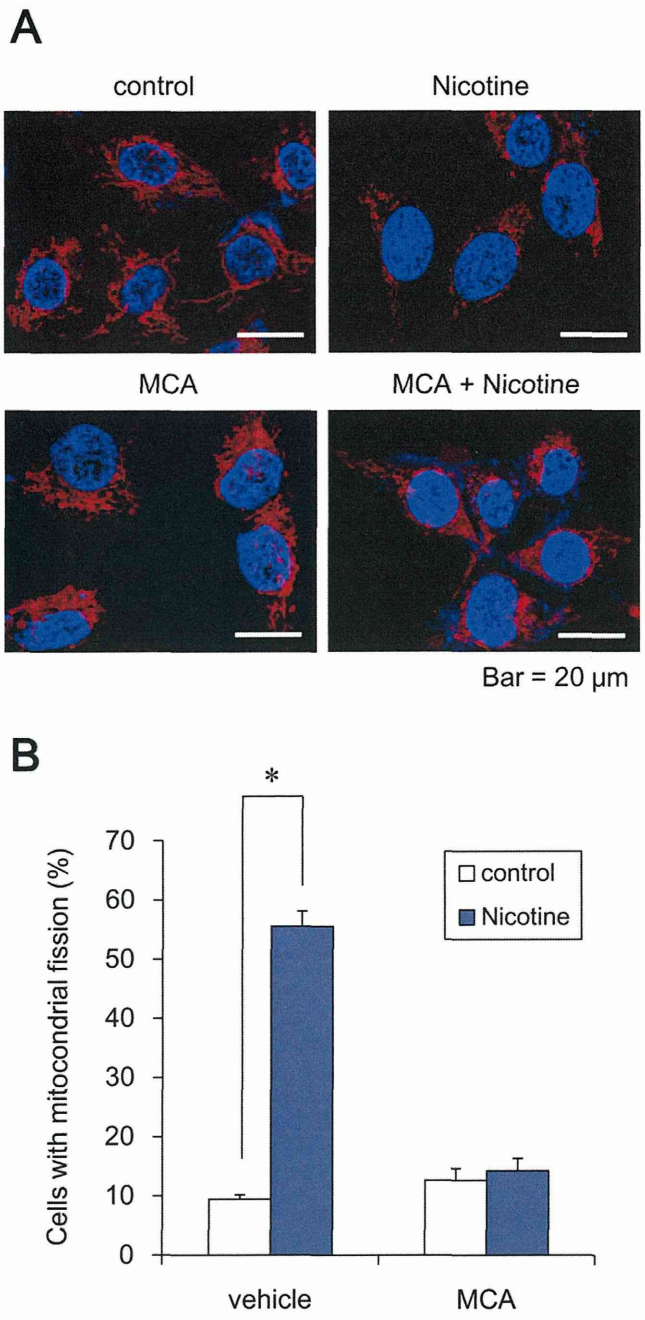

Fig. 3. Nicotine induces mitochondrial fission via nAChRs in NT2/D1 cells. A. Cells were exposed to 10 μM nicotine, in the presence or absence of 30 μM MCA, for 24 h. The cells were stained with MitoTracker Red CMXRos and DAPI and mitochondrial morphology was observed by confocal laser microscopy. Bar = 20 μm. B. The number of cells showing mitochondrial fusion (<10% punctiform) was counted in three independent captured images. The number of cells showing mitochondrial fission was calculated by subtracting the number of cells with mitochondrial fusion from the total cell number. *P < 0.05.

production is mediated via the nAChRs, we tested the effect of nAChR antagonist on the ATP content. As shown in Fig. 2B, a non-selective nAChR antagonist mecamylamine (MCA) abolished the nicotine-induced reduction of ATP content. MCA alone did not affect the ATP level. These data suggest that nicotine decreases the ATP content via its nAChR and inhibits cell proliferation in NT2/D1 cells.

3.2. Effects of nicotine on mitochondrial morphology in NT2/D1 cells

Mitochondrial function, including ATP production, are maintained by mitochondrial fusion and fission [11]. Since nicotine reduced intracellular ATP levels, we next focused on the mitochondrial dynamics in NT2/D1 cells. Nicotine exposure (10 μM, 24 h) significantly increased the number of fragmented mitochondria with punctate morphology, as compared to the level observed in untreated control cells (Fig. 3). Moreover, MCA abolished this nicotine-induced mitochondrial fragmentation (Fig. 3). MCA alone did not affect mitochondrial dynamics. In contrast to NT2/D1 cells, nicotine did not significantly affect the mitochondrial dynamics in SH-SY5Y neuroblastoma cells (Fig. S1). These results suggest that nicotine induces mitochondrial fission via nAChRs in NT2/D1 cells.

3.3. Nicotine reduces Mfn1 and Mfn2 protein levels in NT2/D1 cells

To examine the molecular mechanism by which nicotine induces mitochondrial fragmentation, we assessed its effects on mitochondrial fission (Fis1, Drp1) and fusion genes (Mfn1, Mfn2, Opa1). Real-time PCR analysis showed that each gene expression was not significantly altered by nicotine exposure (Fig. 4A). Interestingly, western blot analysis revealed that nicotine did significantly decrease the levels of Mfn1 and Mfn2 proteins (Fig. 4B and C). In contrast, the levels of other proteins, including Fis1, Drp1, and Opa1, were not affected by nicotine. These data suggest that nicotine-induced mitochondrial fragmentation is caused by the degradation of Mfn1 and Mfn2 proteins.

4. Discussion

In the present study, we demonstrated that exposure to micromolar levels of nicotine impairs mitochondrial quality control in human multipotent embryonic carcinoma cells. Exposure to nicotine induces nAChR-dependent degradation of Mfn1 and Mfn2, thereby promoting mitochondrial fragmentation. These negative nAChR-mediated effects of nicotine on mitochondrial quality control could inhibit ATP production and cell viability.

Undifferentiated embryonic cells may tend to be sensitive to the growth inhibitory effects of nicotine, whereas proliferative and protective effects of nicotine have been described in more developed somatic cells [23–27]. Our studies showed that treatment with 10 μM nicotine reduces cell growth in human embryonic cells (Fig. 1), whereas the growth of human neuroblastoma SH-SY5Y cells is not affected (Fig. S1). Previous study has also shown that exposure to more than 1.8 μM nicotine inhibits cell adhesion and induces apoptosis in human embryonic stem cells [28]. The concentrations of nicotine tested in our study were relevant to the circulating levels of nicotine in cigarette smokers, which have been reported to range from 10 nM to 10 μM [29]; these have the potential to inhibit the growth of embryonic cells. In contrast to these growth inhibitory effects, nicotine is known to stimulate the proliferation of hematopoietic and neuronal progenitors [23–25]. In addition, nicotine is reported to protect rat basal forebrain neurons or rat hippocampal neurons from the cytotoxicity of β-amyloid protein [26,27]. Taken together, nicotine effects in undifferentiated embryonic cells contains different mechanisms from developed somatic cells. Therefore, further studies are required to elucidate the mechanism of cell stage-specific effects using embryonic and differentiated cells.

Our data suggest that nicotine induces mitochondrial fission through the degradation of Mfn1 and Mfn2 (Figs. 3 and 4). Consistent with this finding, chemical stressors have been reported

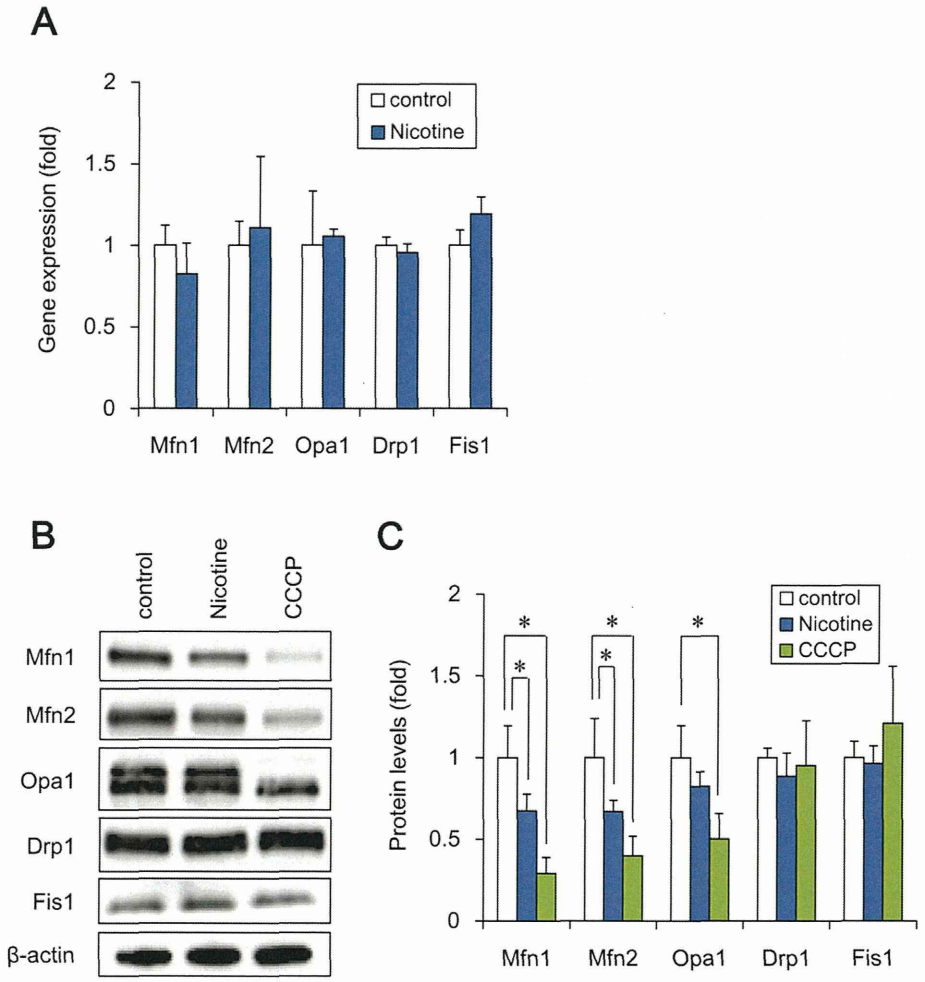

Fig. 4. Nicotine reduces Mfn1 and Mfn2 protein levels in NT2/D1 cells. A. After exposure to 10 μM nicotine for 24 h, the expression of the indicated mitochondrial genes was analyzed by real-time PCR. The relative changes were determined by normalizing with GAPDH. B. After exposure to 10 μM nicotine or 10 μM CCCP for 24 h, the expression of mitochondrial proteins was analyzed by western blot using anti-Drp1, anti-Fis1, anti-Mfn1, anti-Mfn2, anti-Opa1, or anti-β-actin antibodies. C. The band densities were analyzed by ImageJ software. Relative changes in expression were determined by normalization to β-actin. Data represent the mean ± SD (n = 3). *P < 0.05.

to cause mitochondrial fission via Mfn degradation. For example, organotin compounds such as tributyltin induce proteasomal degradation of Mfn1 and Mfn2, which facilitates mitochondrial fragmentation and growth arrest in NT2/D1 cells [30,31]. Since nicotine showed similar effects in NT2/D1 cells, nicotine exposure may also degrade Mfn1 and Mfn2 via proteasome. Moreover, an inhibitor of mitochondrial calcium efflux, CGP37157, is reported to degrade Mfn1 via E3 ubiquitin ligase and induce mitochondrial fission in prostate cancer LNCaP cells [32]. Further studies will be necessary to determine whether ubiquitin ligases are involved in nicotine-induced Mfn1 and Mfn2 degradation in embryonic cells.

Our data suggest that nicotine toxicity is mediated by dysfunctional mitochondrial quality control, which occurs via a nAChR-dependent mechanism (Figs. 2 and 3). Nicotine has been reported to evoke extracellular calcium influx through plasma membrane nAChRs [4]. Moreover, a transient increase in intracellular calcium levels is known to cause mitochondrial calcium overload, which is followed by the depolarization of the mitochondrial membrane, resulting in a loss of MMP [33,34]. In other cell lines, MMP reduction is reported to induce the mitochondrial translocation of the E3 ubiquitin ligase, Parkin, which targets the Mfn protein for proteasomal degradation [35]. Therefore, nicotine may increase intracellular calcium entry via nAChRs, thus reducing the MMP and inducing mitochondrial translocation of E3 ubiquitin ligases; this increases the proteasomal degradation of Mfn1 and Mfn2. Several reports indicate that knockdown of Mfn1 and Mfn2 in the cells induces mitochondrial fragmentation and shows severe cellular defects, including decreased ATP content and poor cell growth [36,37]. Especially, Mfn2 has been reported to be necessary for striatal axonal projections of midbrain dopamine neurons by the studies using dopamine neuron-specific Mfn2 knockout mice [38]. Taken together, Mfn1 and Mfn2 might be involved in several nAChR-mediated effects of nicotine, such as the reduction of ATP content, growth inhibition, and modulation of synaptic transmission. In future studies, it will be necessary to investigate the precise mechanism involved in nicotine-induced Mfn degradation, which results in mitochondrial fission and impaired function.

Conflict of interest

The authors declare that there are no conflicts of interest.

Acknowledgments

This work was supported by a Health and Labour Sciences Research Grant from the Ministry of Health, Labour and Welfare,

Japan (#H25-Kagaku-Ippan-002 to Y. Kanda), a Grant-in-Aid for Scientific Research from the Ministry of Education, Culture, Sports, Science, and Technology, Japan (#26293056, #26670041 to Y. Kanda), the Research on Regulatory Harmonization and Evaluation of Pharmaceuticals, Medical Devices, Regenerative and Cellular Therapy Products, Gene Therapy Products, and Cosmetics from Japan Agency for Medical Research and development, AMED (to Y. Sekino), and a grant from the Smoking Research Foundation (Y. Kanda).

Transparency document

Transparency document related to this article can be found online at http://dx.doi.org/10.1016/j.bbrc.2016.01.063.

Appendix A. Supplementary data

Supplementary data related to this article can be found at http://dx.doi.org/10.1016/j.bbrc.2016.01.063.

References

[1] V.S. Knopik, Maternal smoking during pregnancy and child outcomes: real or spurious effect? Dev. Neuropsychol. 34 (2009) 1–36.
[2] C.M. Tiesler, J. Heinrich, Prenatal nicotine exposure and child behavioural problems, Eur. Child. Adolesc. Psychiatry 23 (2014) 913–929.
[3] B.M. Conti-Fine, D. Navaneetham, S. Lei, A.D. Maus, Neuronal nicotinic receptors in non-neuronal cells: new mediators of tobacco toxicity? Eur. J. Pharmacol. 393 (2000) 279–284.
[4] E.X. Albuquerque, E.F. Pereira, M. Alkondon, S.W. Rogers, Mammalian nicotinic acetylcholine receptors: from structure to function, Physiol. Rev. 89 (2009) 73–120.
[5] Y. Kanda, Y. Watanabe, Nicotine-induced vascular endothelial growth factor release via the EGFR-ERK pathway in rat vascular smooth muscle cells, Life Sci. 80 (2007) 1409–1414.
[6] N. Hirata, Y. Sekino, Y. Kanda, Nicotine increases cancer stem cell population in MCF-7 cells, Biochem. Biophys. Res. Commun. 403 (2010) 138–143.
[7] N.L. Benowitz, Pharmacology of nicotine: addiction, smoking-induced disease, and therapeutics, Annu. Rev. Pharmacol. Toxicol. 49 (2009) 57–71.
[8] J.B. Dwyer, S.C. McQuown, F.M. Leslie, The dynamic effects of nicotine on the developing brain, Pharmacol. Ther. 122 (2009) 125–139.
[9] C.L. Crowley-Weber, K. Dvorakova, C. Crowley, H. Bernstein, C. Bernstein, H. Garewal, C.M. Payne, Nicotine increases oxidative stress, activates NF-kappaB and GRP78, induces apoptosis and sensitizes cells to genotoxic/xenobiotic stresses by a multiple stress inducer, deoxycholate: relevance to colon carcinogenesis, Chem. Biol. Interact. 145 (2003) 53–66.
[10] J.E. Bruin, M.A. Petre, S. Raha, K.M. Morrison, H.C. Gerstein, A.C. Holloway, Fetal and neonatal nicotine exposure in wistar rats causes progressive pancreatic mitochondrial damage and beta cell dysfunction, PLoS One 3 (2008) e3371.
[11] R.J. Youle, A.M. van der Bliek, Mitochondrial fission, fusion, and stress, Science 337 (2012) 1062–1065.
[12] T. Koshiba, S.A. Detmer, J.T. Kaiser, H. Chen, J.M. McCaffery, D.C. Chan, Structural basis of mitochondrial tethering by mitofusin complexes, Science 305 (2004) 858–862.
[13] S. Cipolat, O.M. De Brito, B. Dal Zilio, L. Scorrano, OPA1 requires mitofusin 1 to promote mitochondrial fusion, Proc. Natl. Acad. Sci. U. S. A. 101 (2004) 15927–15932.
[14] E. Smirnova, L. Griparic, D.-L. Shurland, A.M. van der Bliek, Dynamin-related protein Drp1 is required for mitochondrial division in mammalian cells, Mol. Biol. Cell 12 (2001) 2245–2256.
[15] Y. Yoon, E.W. Krueger, B.J. Oswald, M.A. McNiven, The mitochondrial protein hFis1 regulates mitochondrial fission in mammalian cells through an interaction with the dynamin-like protein DLP1, Mol. Biol. Cell 23 (2003) 5409–5420.
[16] Y. He, K.W. Leung, Y. Ren, J. Pei, J. Ge, J. Tombran-Tink, PEDF improves mitochondrial function in RPE cells during oxidative stress, Investig. Ophthalmol. Vis. Sci. 55 (2014) 6742–6755.
[17] G.P. Leboucher, Y.C. Tsai, M. Yang, K.C. Shaw, M. Zhou, T.D. Veenstra, M.H. Glickman, A.M. Weissman, Stress-induced phosphorylation and proteasomal degradation of mitofusin 2 facilitates mitochondrial fragmentation and apoptosis, Mol. Cell 47 (2012) 547–557.
[18] S. Yamada, Y. Kotake, Y. Sekino, Y. Kanda, AMP-activated protein kinase-mediated glucose transport as a novel target of tributyltin in human embryonic carcinoma cells, Metallomics 5 (2013) 484–491.
[19] S. Yamada, Y. Kotake, Y. Demizu, M. Kurihara, Y. Sekino, Y. Kanda, NAD-dependent isocitrate dehydrogenase as a novel target of tributyltin in human embryonic carcinoma cells, Sci. Rep. 4 (2014) 5952.
[20] X. Fan, R. Hussien, G.A. Brooks, H_2O_2-induced mitochondrial fragmentation in C2C12 myocytes, Free Radic. Biol. Med. 49 (2010) 1646–1654.
[21] N. Hirata, S. Yamada, T. Shoda, M. Kurihara, Y. Sekino, Y. Kanda, Sphingosine-1-phosphate promotes expansion of cancer stem cells via S1PR3 by a ligand-independent Notch activation, Nat. Commun. 5 (2014) 4806.
[22] Y. Kanda, T. Hinara, S.W. Kang, Y. Watanabe, Reactive oxygen species mediate adipocyte differentiation in mesenchymal stem cells, Life Sci. 89 (2011) 250–258.
[23] M.V. Skok, R. Grailhe, F. Agenes, J.P. Changeux, The role of nicotinic receptors in B-lymphocyte development and activation, Life Sci. 80 (2007) 2334–2336.
[24] L.M. Koval, A.S. Zverkova, R. Grailhe, Y.N. Utkin, V.I. Tsetlin, S.V. Komisarenko, M.V. Skok, Nicotinic acetylcholine receptors alpha4beta2 and alpha7 regulate myelo- and erythropoiesis within the bone marrow, Int. J. Biochem. Cell Biol. 40 (2008) 980–990.
[25] N. He, Z. Wang, Y. Wang, H. Shen, M. Yin, ZY-1, a novel nicotinic analog, promotes proliferation and migration of adult hippocampal neural stem/progenitor cells, Cell Mol. Neurobiol. 33 (2013) 1149–1157.
[26] C.N. Guo, L. Sun, G.L. Liu, S.J. Zhao, W.W. Liu, Y.B. Zhao, Protective effect of nicotine on the cultured rat basal forebrain neurons damaged by β-Amyloid (Aβ)25-35 protein cytotoxicity, Eur. Rev. Med. Pharmacol. Sci. 19 (2015) 2964–2972.
[27] Q. Liu, B. Zhao, Nicotine attenuates beta-amyloid peptide-induced neurotoxicity, free radical and calcium accumulation in hippocampal neuronal cultures, Br. J. Pharmacol. 141 (2004) 746–754.
[28] T. Zdravkovic, O. Genbacev, N. LaRocque, M. McMaster, S. Fisher, Human embryonic stem cells as a model system for studying the effects of smoke exposure on the embryo, Reprod. Toxicol. 26 (2008) 86–93.
[29] E.R. Gritz, V. Baer-Weiss, N.L. Benowitz, M.E. Van VunakisHjarvik, Plasma nicotine and cotine concentrations in habitual smokeless tobacco users, Clin. Pharmacol. Ther. 30 (1981) 201–209.
[30] S. Yamada, Y. Kotake, M. Nakano, Y. Sekino, Y. Kanda, Tributyltin induces mitochondrial fission through NAD-IDH dependent mitofusin degradation in human embryonic carcinoma cells, Metallomics 7 (2015) 1240–1246.
[31] M. Asanagi, S. Yamada, N. Hirata, H. Itagaki, Y. Kotake, Y. Sekino, Y. Kanda, Tributyltin induces G2/M cell cycle arrest via NAD^+-dependent isocitrate dehydrogenase in human embryonic carcinoma cells, J. Toxicol. Sci. (2016) in press.
[32] V. Choudhary, I. Kaddour-Djebbar, R. Alaisami, M.V. Kumar, W.B. Bollag, Mitofusin 1 degradation is induced by a disruptor of mitochondrial calcium homeostasis, CGP37157: a role in apoptosis in prostate cancer cells, Int. J. Oncol. 44 (2014) 1767–1773.
[33] M.R. Duchen, Mitochondria and calcium: from cell signalling to cell death, J. Physiol. 529 (2000) 57–68.
[34] N. Demaurex, D. Poburko, M. Frieden, Regulation of plasma membrane calcium fluxes by mitochondria, Biochim. Biophys. Acta 1787 (2009) 1383–1394.
[35] A. Tanaka, M.M. Cleland, S. Xu, D.P. Narendra, D.F. Suen, M. Karbowski, R.J. Youle, Proteasome and p97 mediate mitophagy and degradation of mitofusins induced by Parkin, J. Cell Biol. 191 (2010) 1367–1380.
[36] H. Chen, A. Chomyn, D.C. Chan, Disruption of fusion results in mitochondrial heterogeneity and dysfunction, J. Biol. Chem. 280 (2005) 26185–26192.
[37] W. Yue, Z. Chen, H. Liu, C. Yan, M. Chen, D. Feng, C. Yan, H. Wu, L. Du, Y. Wang, J. Liu, X. Huang, L. Xia, L. Liu, X. Wang, H. Jin, J. Wang, Z. Song, X. Hao, Q. Chen, A small natural molecule promotes mitochondrial fusion through inhibition of the deubiquitinase USP30, Cell Res. 24 (2014) 482–496.
[38] S. Lee, F.H. Sterky, A. Mourier, M. Terzioglu, S. Cullheim, L. Olson, N.G. Larsson, Mitofusin 2 is necessary for striatal axonal projections of midbrain dopamine neurons, Hum. Mol. Genet. 21 (2012) 4827–4835.

〈レクチャー6-3〉ファーマコビジランス

ヒトiPS細胞を用いた心毒性試験の現状と課題

諫田　泰成
国立医薬品食品衛生研究所・薬理部第二室

1. はじめに

ヒトiPS細胞の心毒性試験は、モデルとなる分化細胞を作製して医薬品候補化合物のスクリーニングを*in vitro*アッセイ系で評価することになるので、ヒト心筋を反映するような分化心筋細胞が大量かつ安定的に供給されることが必要不可欠である。現在、ヒトiPS細胞には株間の差など様々なバリエーションが存在することが明らかになっていることから[1]、分化誘導した心筋細胞にも未分化iPS細胞と同様にバラつきがあると考えられる。しかしながら、分化心筋細胞の品質基準などは定まっておらず、アカデミアやメーカーにおいてそれぞれバラバラの細胞を用いてアッセイを行っている可能性がある。インハウスの試験法を行う場合には問題はないが、安全性試験を実施するためには一定の評価基準が必要である。幹細胞由来の分化細胞は培養期間によっても性質が変化しうることが分かってきており、株化細胞やhERGを過剰発現させたHEK293細胞などのように扱うことができない。従って、いかに分化心筋細胞の品質を確保するのかが重要である。

本稿では、ヒトiPS細胞から心筋細胞への分化誘導技術ならびにiPS由来分化心筋細胞の薬理学的な特性を概説し、今後、医薬品による催不整脈作用に対する応用可能性、さらにはICHガイドラインへの展望について議論したい。

2. 医薬品による催不整脈作用

医薬品によって発生する副作用の中で、トルサード・ド・ポアント(TdP)とよばれる重篤な不整脈は重要である[2]。発生頻度は極めて少ないものの心室細動に移行し突然死に至る症例が報告されており、上市後に販売が中止になった医薬品も少なくない。TdPはQT間隔の延長を伴うことから、TdP誘発リスクは、非臨床試験として*in vitro*でカリウム電流(hERGチャネル)阻害作用および*in vivo*で動物におけるQT延長作用を評価し(S7Bガイドライン)、臨床においてThorough QT/QTc試験を実施して厳密にヒトのQT間隔に対する作用を調べて(E14ガイドライン)、総合的にTdP誘発リスクを評価している。これらのガイドラインが整備された後は薬剤性心毒性の大きな問題は起きていないことから、一定のリスク評価ができていると考えられる。しかしながら、hERG試験で有用な医薬品候補化合物を落としてしまうこと、逆にhERGだけでは拾えない不整脈作用があることなどが指摘され、さらに予測性の高い試験系が求められている。iPS由来分化心筋細胞はヒト細胞でありマルチチャネルに対する評価が可能であることから[3]、hERG試験よりも予測性が向上するのではないか、あるいは臨床試験を削減できるのではないか、との期待が寄せられている。

3. ヒトiPS細胞を用いた心筋分化誘導法

ヒトiPS細胞を効率よく心筋分化する方法として、定方向分化誘導法が知られている[3,4]。**図1**に示すように、ヒトiPS細胞にサイトカインや増殖因子などを用いることにより、中胚葉、心筋前駆細胞、心筋細胞と段階的に分化誘導を行い、分化誘導後2週間ほどで自律的な拍動が観察される。このように作成されたiPS由来分化心筋細胞は個々の心筋細胞の活動電位の波形がバラバラである上に、電気生理学的に未成熟である。実際、201B7株から作製した分化心筋細胞も米国Cellular Dynamics International Inc.(CDI)から販売されているiCell心筋細胞も静止膜電位は-50mV程度と浅い(通常-90mV程度)。従って、未成熟な特性は元のiPS細胞株や分化誘導法に依存せず、iPS由来分化心筋細胞に共通の課題であることが示唆される。

そこで、心筋の成熟化を促進するためのアプローチとして、電気刺激など様々な手法が検討されてい